

Review

Open Access



Recent prospects, challenges and advancements of photocatalysis as a wastewater treatment method

Paraskevi Chalatsi-Diamanti, Ekavi Aikaterini Isari, Eleni Grilla, Petros Kokkinos , Ioannis K. Kalavrouziotis

Laboratory of Sustainable Waste Management Technologies, School of Science and Technology, Hellenic Open University, Patras 26335, Greece.

Correspondence to: Assoc. Prof. Petros Kokkinos, Laboratory of Sustainable Waste Management Technologies, School of Science and Technology, Hellenic Open University, Parodos Aristotelous 18, Patras 26335, Greece. E-mail: pkokkin@eap.gr

How to cite this article: Chalatsi-Diamanti, P.; Isari, E. A.; Grilla, E.; Kokkinos, P.; Kalavrouziotis, I. K. Recent prospects, challenges and advancements of photocatalysis as a wastewater treatment method. *Water Emerg. Contam. Nanoplastics* 2025, 4, 12. <https://dx.doi.org/10.20517/wecn.2025.03>

Received: 24 Feb 2025 **First Decision:** 22 Apr 2025 **Revised:** 16 May 2025 **Accepted:** 27 May 2025 **Published:** 30 May 2025

Academic Editor: Joana C Prata **Copy Editor:** Pei-Yun Wang **Production Editor:** Pei-Yun Wang

Abstract

The climate crisis, unrestrained use of water resources, and rising population demands have amplified the urgency for sustainable and eco-friendly wastewater treatment solutions. Conventional methods often fail to degrade emerging and persistent pollutants produced by industries, driving the need for alternative technologies. In this context, photocatalysis has emerged as a promising and effective method, offering superior degradation of contaminants and cost-effective application, especially with its advancements in recent years. As an advanced oxidation process (AOP), photocatalysis is particularly well-suited to address the limitations of traditional treatments. This review paper explores the types of photocatalysts and their operational mechanisms, examines the key parameters affecting degradation efficiency, such as operating conditions and photoreactor design, and analyzes recent developments in wastewater effluents containing emerging contaminants over the past five years. Lastly, this review proposes the integration of photocatalysis with other treatment technologies and presents potential future directions for research.

Keywords: Photocatalysis, wastewater treatment, emerging contaminants, photoreactors, combined technologies, future direction



© The Author(s) 2025. **Open Access** This article is licensed under a Creative Commons Attribution 4.0 International License (<https://creativecommons.org/licenses/by/4.0/>), which permits unrestricted use, sharing, adaptation, distribution and reproduction in any medium or format, for any purpose, even commercially, as long as you give appropriate credit to the original author(s) and the source, provide a link to the Creative Commons license, and indicate if changes were made.



INTRODUCTION

The global climate crisis, coupled with rapid industrialization, urbanization, and unsustainable water consumption, has placed immense pressure on existing water systems. As freshwater resources become increasingly scarce, sustainable wastewater treatment methods are urgently needed^[1,2]. In recent years, emerging contaminants (ECs), including pesticides, pharmaceuticals, microplastics, and industrial chemicals, pose a growing concern due to the lack of regulations for monitoring or reporting their presence in water supplies. Municipal wastewater contributes significantly to EC pollution, with conventional wastewater treatment plants (WWTPs) being unable to remove these pollutants effectively^[3].

To address these challenges, novel and combined treatment methods have recently been developed and tested at laboratory and pilot scales for enhanced removal of ECs and persistent organic pollutants (POPs) in various wastewater effluents. Some of the proposed methods include physicochemical processes, absorption, membrane filtration, ozonation, electrochemical processes, biological treatment, advanced oxidation processes (AOPs), and others^[4,5]. Among these, AOPs have emerged as highly effective wastewater treatment methods due to their ability to generate highly reactive hydroxyl radicals ($\cdot\text{OH}$), which degrade a wide range of organic pollutants, including pharmaceuticals, pesticides, and industrial chemicals. AOPs encompass techniques such as ozonation, reagent activation processes, Fenton oxidation, electrodeionization, electrochemical processes, and photocatalysis. Their main advantages include high removal efficiency, wide-spectrum pollutant degradation, minimal sludge generation, and pathogen inactivation^[6].

However, each AOP has intrinsic limitations. For example, ozonation, while capable of generating strong oxidants and enabling fast degradation, involves high operational costs due to the energy required for ozone generation and the need for specialized equipment. Fenton processes require strictly acidic conditions, which limits their applicability in neutral or alkaline wastewater. Additionally, they produce iron-containing sludge, which needs further treatment before disposal, thereby increasing the operational complexity. Electrochemical oxidation, which relies on electrical current to drive redox reactions, leads to challenges such as high energy consumption, scalability issues due to frequent maintenance, and electrode replacement costs^[6].

In contrast, photocatalysis stands out for its ability to offset most of these drawbacks due to its efficiency, development potential, and adaptability. It operates under mild conditions and can utilize natural sunlight, making it a more energy-efficient and cost-effective approach in the long term compared to other AOPs, such as ozonation or electrochemical oxidation. Unlike the Fenton process, photocatalysis avoids secondary sludge production and enables the reusability of the catalysts. Additionally, the synthesis and use of low-cost, non-toxic, visible light active and stable semiconductor photocatalysts reinforce its viability, especially when photocatalysis is activated by solar energy^[7]. In terms of by-product formation, photocatalysis typically results in fewer harmful intermediates due to the mineralization pathways, whereas ozonation can generate more toxic intermediates if not properly controlled. [Figure 1](#) provides a conceptual overview of the photocatalytic process and the scope of this review.

This review discusses the progress made over the past five years in the development of novel photocatalysts, the design of photoreactors, the removal efficiency of ECs, and treatment conditions for various wastewater effluents. Additionally, it provides an overview of combined technologies aimed at minimizing drawbacks and accelerating large-scale applications. Finally, it highlights future research prospects, hoping to inspire and generate ideas for overcoming the challenges faced during the implementation of photocatalysis in real-life wastewater treatment.

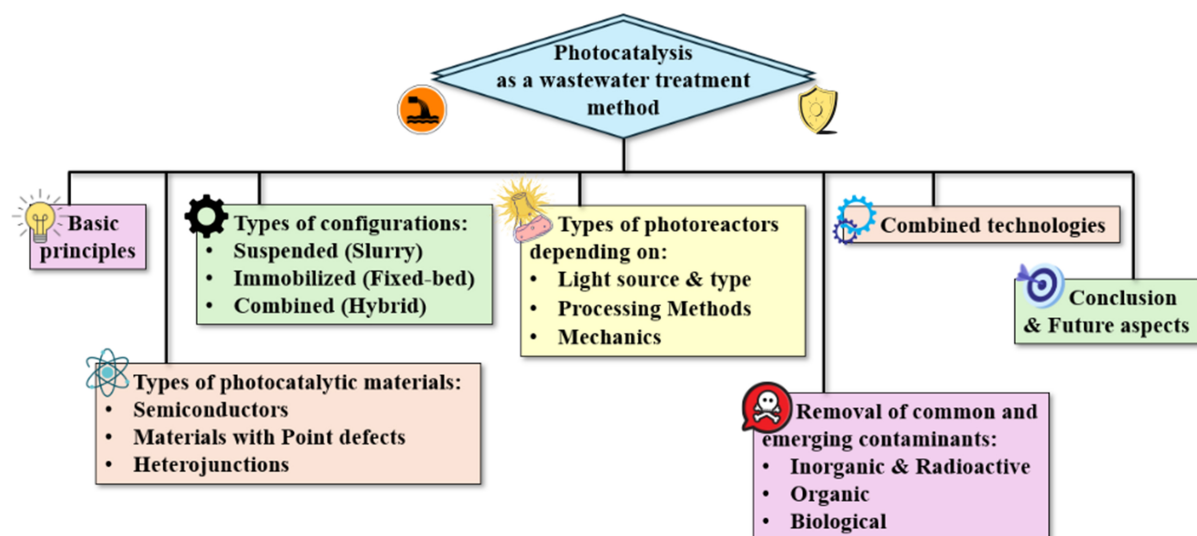


Figure 1. Schematic diagram highlighting the contents of this review.

BASIC PRINCIPLES OF PHOTOCATALYSIS - MECHANISM

The photocatalysis mechanism is based on a light source for energy and a photocatalytic material as a “mediator” to accelerate a chemical reaction, while remaining unconsumed. When a photocatalyst, typically a semiconductor, absorbs photons with energy equal to or greater than its band gap (E_g), an electron (e^-) from the valence band (VB) gets excited and moves to the conduction band (CB). This transfer results in a positively charged hole (h^+) in the VB. A narrower band gap increases electron-hole pair generation^[8].

For effective photocatalysis, electron-hole recombination must be minimized. Strategies such as doping, introducing surface defects, or coupling with other catalysts enhance charge separation and electron transfer to reactive sites^[9,10]. The excited electrons in the CB act as reductants, while holes in the VB facilitate oxidation. These species generate reactive oxygen species (ROS) such as $\cdot\text{OH}$ and superoxide anions ($\text{O}_2^{\cdot-}$), which degrade organic pollutants^[8].

In wastewater treatment, pollutants adsorb on the photocatalyst surface, where ROS drive reactions that break them down into less harmful by-products^[9,11]. Moreover, a noteworthy variant of the photocatalytic process is the photo-Fenton process, which enhances ROS production via Fe^{2+} and hydrogen peroxide (H_2O_2), yielding additional $\cdot\text{OH}$ ^[12].

An optimal photocatalyst should be efficient, non-costly, environmentally friendly, stable, and sunlight-activated.

Key attributes include eco-friendly synthesis, a narrow band gap for visible light activation, low electron-hole recombination, structural stability, resistance to leaching, high surface area, and strong reactivity. Additionally, it should effectively degrade pollutants into non-toxic by-products, be easily separated from treated water and retain activity over multiple cycles while minimizing reliance on UV light^[10,11,13].

Several parameters influence photocatalytic efficiency. Contact time and catalyst dose impact degradation efficiency, as longer exposure enhances pollutant removal until saturation, while excessive catalyst loading can reduce efficiency due to light scattering and particle aggregation. Light intensity and wavelength also

play a crucial role. While UV light is most commonly used, recent efforts have focused on developing visible-light-active catalysts to reduce energy costs^[13-16]. The pH of the solution affects both the photocatalyst surface charge and the degradation pathways. When the pH is below the point of zero charge (PZC), the surface becomes positively charged, attracting anionic pollutants, while at pH above PZC, the surface is negatively charged, attracting cationic pollutants^[16]. pH also influences the generation of ROS, such as $\cdot\text{OH}$ and $\text{O}_2^{\cdot-}$, with lower pH favoring their production. Additionally, the stability and performance of the photocatalyst are pH-dependent; extremely high pH levels can negatively affect both the catalyst and its degradation efficiency^[13]. Temperature plays a significant role in photocatalytic degradation. Although most reactions are conducted at room temperature, studies show that temperatures below 0 °C slow the reaction rate, while excessively high temperatures can degrade the photocatalyst and shorten the lifetime of reactive species. In contrast, moderate temperatures generally accelerate reaction kinetics by enhancing charge carrier generation and improving adsorption^[13,17]. Oxidizing agents can improve photocatalytic degradation by promoting ROS formation and enhancing electron-hole pair dynamics. However, their concentration should be carefully controlled, as excessive amounts could break down the catalyst^[13,18]. In real wastewater systems, inorganic ions may interfere with photocatalytic reactions by altering pH, scavenging reactive species, or occupying active sites on the catalyst surface. Some ions can even induce photocatalyst aggregation, thereby reducing its efficiency^[17,19]. The concentration of pollutants also influences photocatalytic degradation rates. At lower concentrations, degradation is typically faster due to the abundance of available active sites and reactive species. In contrast, higher pollutant concentrations can hinder degradation, mainly due to the difficulty of light penetration, leading to a reduction in accessible active sites^[13].

TYPE OF PHOTOCATALYTIC MATERIALS

Photocatalytic materials are primarily used to accelerate chemical reactions when exposed to light. A wide variety of these materials exist, and new ones are continuously being developed to enhance efficiency and minimize drawbacks. They can be categorized based on their composition, structure, or combination with other compounds. Broadly, photocatalytic materials can be classified into semiconductors, materials with point defects, and heterojunctions.

Semiconductors

Semiconductors are the earliest and most widely used photocatalytic materials due to their stability and high photocatalytic ability. Commonly used examples include ZnO, TiO₂, Cu₂O, MgO, and SnO₂. However, conventional semiconductors typically require UV light or activation because of their large band gaps, while UV light accounts for only 5% of the solar spectrum. In comparison to visible light, UV radiation is not only more harmful to human health but also significantly more costly to generate. To address these challenges, research has increasingly focused on developing semiconductors that can be activated by visible light. However, visible-light-responsive semiconductors, which generally have narrower band gaps, often suffer from high rates of electron-hole pair recombination, reducing their efficiency in pollutant degradation. To overcome this limitation, various strategies have been developed, leading to many categories of photocatalysts for wastewater treatment^[20]. For instance, Bahadoran *et al.* proposed using e-waste as a source of raw materials for synthesizing photocatalysts, thereby enhancing both reusability and sustainability^[21]. Similarly, Chen *et al.* suggested recovering metals from e-waste by exploiting the catalytic properties of these photocatalysts^[22].

Another challenge in semiconductor photocatalysis is photocorrosion, where prolonged light exposure degrades the material itself. This not only shortens the lifespan and reduces the stability of the semiconductor but can also lead to secondary water contamination from the degraded material. To mitigate

this issue, oxide semiconductors are often preferred for their exceptional electrical and physical stability under illumination^[23].

Materials with point defects

The simplest way to enhance the degradation ability of a semiconductor is by introducing point defects in its structure. These defects refer to imperfections occurring at a single location or/and on a minor scale within the crystal lattice, and they can significantly influence the material's photocatalytic properties. However, the greater the amount of point defects, the greater the instability of the photocatalyst. Defects can arise from an atom's complete vacancy or variation from its conventional lattice position, exchange of the atoms with others, or doping with foreign elements^[24]. These structural modifications introduce additional energy levels, allowing electron excitation and transfer to the CB. Hence, the band gap energy limitation can be overcome, enabling the defective photocatalyst to absorb lower-energy photons and operate with improved efficiency^[23]. Additionally, p-type (positive) and n-type (negative) doping introduces controlled impurities that create an excess of holes (or vacancies) and electrons, respectively.

Several studies have demonstrated the effectiveness of point defects and doping in enhancing photocatalytic performance. Wang *et al.* achieved 100% degradation of perfluorooctanoic acid (PFOA) within 6 h under UV illumination using oxygen vacancy BiOF nanosheets^[25]. In another research, Wu *et al.* utilized oxygen vacancies on the surface of In₂O₃ (MnOx/In₂O₃), achieving 99.8% degradation of PFOA within 3 h under solar light^[26]. Similarly, Núñez-Salas *et al.* doped ZnO with boron (BeZnO), enabling 89% degradation of cyanide under visible light in just 2 h^[27]. Aboutaleb and El-Salam also reported 96% degradation of Congo red (CR) dye within 3 h under visible light by doping CeO₂ nanoparticles (NPs) with Fe^[28].

Heterojunctions

The formation of heterojunctions/heterostructures is attributed to the need to enhance charge separation and minimize electron-hole recombination. Specifically, a heterojunction consists of two distinct semiconductor materials with different band structures. During its formation, the CB and VB align in a specific way at the interface. This alignment allows electron transfer from one material to the other, depending on the relative energy levels of the bands. Since the materials involved vary, their band alignment also differs, leading to^[29] different photocatalytic pathways that reduce electron/hole recombination^[30,31].

Type-I heterojunction

Type-I heterojunction, also known as a straddling type of heterojunction, is characterized by a symmetric arrangement of the CB and VB of the two semiconductors. In this configuration, both the CB and VB of one material (M1) lie at lower energy levels than those of the other material (M2). Consequently, both electrons and holes tend to remain within the same semiconductor, typically the one with the narrower bandgap. As a result, charge carriers are confined within a single material, which limits the efficiency of charge separation and increases the rate of electron-hole recombination^[32]. Khurram *et al.* compared the photocatalytic degradation efficiency of CR using bare α -Fe₂O₃/ZnO and α -Fe₂O₃/ZnSe nanocomposites^[33]. The findings indicated that the degradation efficiency of α -Fe₂O₃/ZnO (Type-I heterojunction) was lower (< 26%) than both the efficiency (98.9%) of α -Fe₂O₃/ZnSe (Type-II heterojunction) and the individual photocatalysts (26% for ZnSe and 43% for α -Fe₂O₃). These results highlight the limited performance of Type-I heterojunctions due to their higher electron-hole recombination rates compared to single semiconductors.

Type-II heterojunction

In a type-II heterojunction, also known as staggered-gap type heterojunction, the CB1 and VB1 of M1 are positioned at lower energy levels than those of the M2. This band alignment drives electrons toward the

lower energy CB1 and holes toward the higher energy VB2. This results in the spatial separation of electrons and holes across the two materials, decreasing recombination and enhancing photocatalytic activity^[34]. Paul *et al.* synthesized a CsPbBrCl₂/g-C₃N₄ heterojunction for the efficient degradation of textile dye Eosin B under visible light irradiation^[35]. Their results showcased an impressive degradation efficiency of 94%, compared to 73% and 86% for the individual components. Moreover, the heterojunction exhibited excellent stability and reusability after testing in 3 consecutive cycles. Another example of type-II heterojunction synthesis and use was implemented by Cui *et al.*, who degraded Rhodamine B (RhB) using In₂S₃/Bi₂MoO₆ under 90 min of visible light illumination^[36]. The degradation efficiency reached 88.2%, which remained above 81.4% even after 4 cycles. However, a notable disadvantage is the reduced charge carrier mobility, which can slow down reaction rates^[23].

Type-III heterojunction

A type-III heterojunction, also known as broken-gap heterojunction, is characterized by the CB1 of M1 being located entirely below the VB2 of M2. This results in a broken band alignment with no direct overlap between the conduction and VBs of the two materials. During light illumination, electrons are excited to the CB1 of M1, while holes are generated in the VB2 of (M2). Due to the broken band alignment, the charge carriers are separated across the materials, and electrons tend to migrate to CB2 (higher-energy CB), while holes move to VB1 (lower-energy VB). Therefore, recombination is minimized, and photocatalytic efficiency is increased by enabling charge carriers to participate in different photocatalytic reactions^[31]. Nevertheless, the broken band alignment of the two combined materials leads to poor electron transfer between them, as there is no continuous energy pathway for electron flow. This may slow carrier dynamics or hinder the mitigation of electrons and holes to their respective reactive sites^[37]. Lastly, type III heterojunctions are generally considered unstable under prolonged irradiation or harsh photocatalytic conditions, limiting their practical applications^[38]. In an effort to overcome these limitations, Li *et al.* proposed incorporating plasmonic metal NPs between the semiconductor components^[39]. This strategy facilitated the selective transfer of photothermally generated electrons and holes, effectively converting the type III catalyst into a type B heterojunction photo-thermo-catalyst and thus achieving a 73-fold enhancement in the photothermocatalytic degradation rate of toluene.

Z-scheme heterojunction

A Z-scheme heterojunction exhibits a band alignment similar to that of a type-II heterojunction, while the key difference lies in their charge transfer mechanisms [Figure 2]^[34].

Jiang *et al.* synthesized the BiFeO₃/ZnFe₂O₄ for the degradation of methylene blue (MB) and tetracycline (TC) under visible light irradiation^[40]. BFO/ZFO-10% achieved the greatest degradation performance on MB and TC. Luo *et al.* used AgI NP/Zn₃V₂O₈ for TC degradation and observed that within 140 min under visible light irradiation, the degradation efficiency reached 91%^[41]. Chen *et al.* studied the photocatalytic degradation of ephedrine (EHP) by AgBr/P-g-C₃N₄^[42]. The results indicated an efficiency of 99.9% in 1 h^[43].

p-n Heterojunction

A p-n heterojunction forms by coupling a p-type with an n-type semiconductor, creating an internal electric field that accelerates charge carrier transfer to the photocatalyst's surface while reducing recombination. Like type-II, redox reactions occur on the surface but with lower oxidation/reduction potentials than Z-scheme systems^[34]. Beshkar *et al.* used a CuI/FePO₄ p-n heterojunction for amoxicillin (AMX) degradation under simulated sunlight, achieving ~90% efficiency versus ~41% (CuI) and ~69% (FePO₄) individually^[44]. Limitations include narrow light absorption and potential band alignment issues that hinder performance^[31].

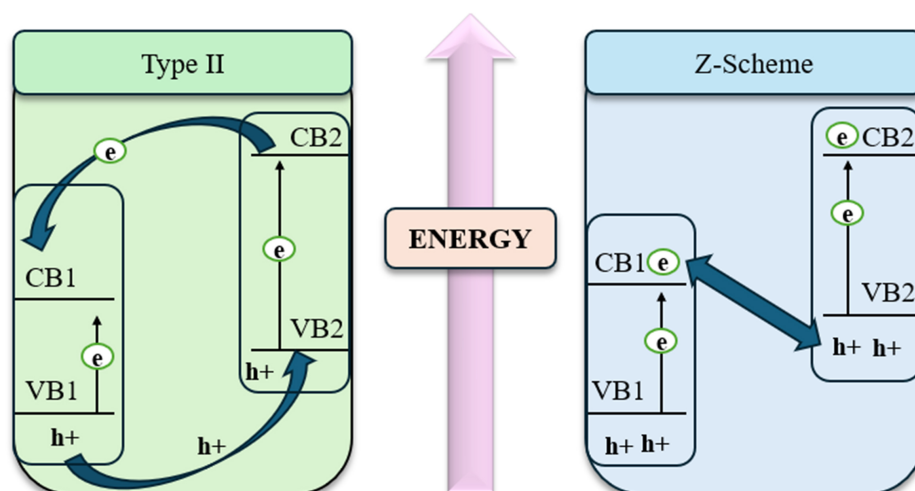


Figure 2. Differences between Z-scheme and Type-II heterojunction mechanisms.

S-scheme heterojunction

S-scheme (step-scheme) heterojunctions combine two n-type semiconductors with a type-II-like band structure but distinct charge transfer. Semiconductor A (SA), with a lower work function, interacts with semiconductor B (SB), causing electron flow from SB to SA and forming an internal field. This leads to band bending, downward in SB and upward in SA. Upon light irradiation, electrons in SB recombine with holes in SA, while the reductive electrons in SA and oxidative holes in SB remain active for surface redox reactions^[31,45]. Fan *et al.* developed $\text{In}_2\text{S}_3/\text{Bi}_2\text{O}_2\text{CO}_3$ S-scheme for RhB degradation, reaching 91% efficiency in 60 min under simulated light^[46]. While efficient, they face limited light absorption and possible charge transfer inefficiencies due to suboptimal band alignment^[45].

Schottky heterojunction

A Schottky heterojunction [Figure 3] forms between a semiconductor and a metal due to their Fermi level difference, creating a Schottky barrier that reduces electron-hole recombination and enhances photocatalytic activity^[47]. Material compatibility is crucial for stability^[48]. Graimed *et al.* synthesized a $\text{SiO}_2/\beta\text{-Bi}_2\text{O}_3/\text{Ag}$ Schottky heterojunction to degrade ciprofloxacin under light-emitting diode (LED) light, achieving 96% efficiency in 105 min, with high stability over five cycles^[49].

While photocatalytic materials present a promising potential for degrading ECs in wastewater, their real-world applicability varies. Semiconductors are effective for degrading pharmaceuticals under UV light, but they face problems such as narrow light absorption ranges and recovery issues. Materials with point defects offer improved visible light activity and charge separation, yet they often suffer from issues related to instability and scalability. In this context, heterojunctions further boost performance by reducing electron-hole recombination, making them suitable for treating complex pollutants. However, they are prone to deactivation and are often expensive to synthesize. It is evident that certain materials perform better for specific contaminants (e.g., g- C_3N_4 -based composites are frequently used for antibiotic degradation)^[42]. Nevertheless, their practical application requires careful optimization tailored to each type of contaminant and the specific characteristics of the water matrix.

TYPES OF PHOTOCATALYTIC CONFIGURATIONS

Photocatalysts can be employed in different configurations to maximize efficiency, depending on the

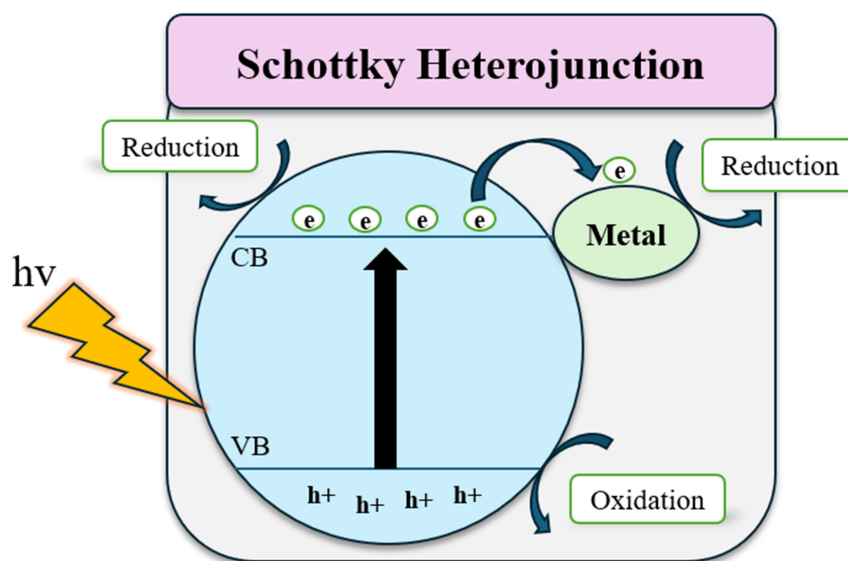


Figure 3. Schematic of the Schottky heterojunction mechanism.

materials used, the matrix, and the type of targeted pollutants. The most common configurations are immobilized systems and suspended (slurry) systems^[50]. When photocatalysis is combined with other techniques or materials, it leads to hybrid systems, such as photoelectrocatalytic (PEC) systems and photocatalytic membrane systems.

Single photocatalysis systems

Immobilized systems

Immobilized photocatalysis (fixed-bed or solid substrate) is one of the earliest and most widely used configurations. In this system, the photocatalyst is fixed onto the surface of a support material, allowing wastewater to flow above or through it. Common support materials include glass, stainless steel, fibers, polymers, silica, ceramic, cellulose, zeolites, metals, photoreactor walls, concrete, aerogels, low-cost substrates, and organometallic frameworks^[51,52]. Upon light exposure, the immobilized catalyst activates and degrades pollutants, offering uniform irradiation, easy catalyst recovery, high reusability (lowers operational costs), and suitability for continuous, large-scale wastewater treatment^[53,54] [Figure 4].

Chairungsri *et al.* immobilized TiO_2 on glass and iron beads to study the photodegradation of textile wastewater in a batch reactor^[55]. These immobilized systems of TiO_2 showed an efficiency of 64% in four hours of irradiation and high reusability in the second cycle. Additionally, Yusuf *et al.* employed an immobilized $\text{TiO}_2/\beta\text{-Bi}_2\text{O}_3$ on borosilicate glass beads for the photocatalytic degradation of diclofenac amide (DCFA) in a recirculating reactor, achieving 90% degradation efficiency after two years of use^[56].

However, there are many challenges present to immobilized systems. First, a considerable part of the surface area of the catalyst is occupied by the support material, limiting its ability to absorb photons and participate in degradation reactions. Second, efficiency may be limited by the reduced contact between pollutants and the photocatalyst surface, especially in low-flow conditions. Limited light penetration can hinder photocatalyst activation in deeper layers, lowering efficiency. Finally, surface fouling by organic/inorganic deposits over time further reduces activity^[50].

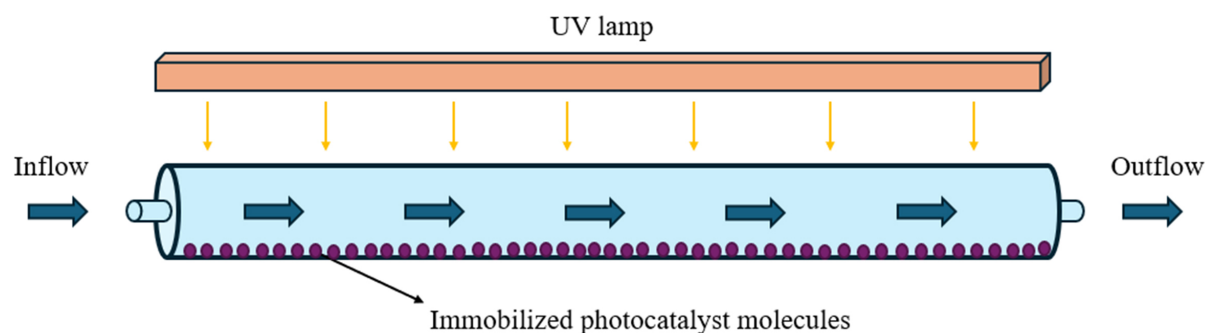


Figure 4. Schematic of a fixed bed photocatalyst reactor.

Suspended (slurry) systems

In suspended systems, powdered photocatalysts disperse in wastewater, maximizing surface area and active site availability for efficient degradation. Another advantage is the flexibility of the system, which can be scaled up or down by adjusting the amount of photocatalyst and light intensity. Moreover, suspended photocatalysts have been proven to be quite useful for degrading a variety of organic pollutants, including those present in complex wastewater matrices^[57].

The disadvantages of the suspended system are related to post-treatment catalyst recovery. Once the degradation process is complete, separating the photocatalyst from the treated water is difficult and often requires filtration or centrifugation, which increases operational costs and leads to catalyst loss over time. Due to their limited reusability, slurry systems are mostly used in laboratory experiments, pilot studies, or novel research setups rather than in large-scale industrial applications. Furthermore, their efficiency tends to decrease over time due to catalyst deactivation and/or fouling [Figure 5].

Al-Tameemi *et al.* investigated the use of suspended SnO_2 as a photocatalyst in a slurry bubble photoreactor for the degradation of COD in petroleum refinery wastewater^[58]. The results indicated the photocatalyst's reusability and the high efficiency of the suspended system (73.16% COD removal in 99 min under optimized conditions) - even suggesting potential for industrial-scale utilization. Shokry *et al.* used commercial TiO_2 to observe the photocatalytic degradation of methyl violet dye^[59]. They concluded that proper adjustment of operational parameters enables effective treatment of low-concentration industrial dye wastewater, with peak degradation at neutral pH (7) before declining at higher values. Ng *et al.* tried to eliminate the need for mechanical stirring, which requires massive amounts of energy for industrial scale-up, by synthesizing a SiO_2 -cored ZnO photocatalyst^[60]. Combined with O_2 -bubbling to maintain particle suspension, their system Combined 67.6% degradation of MB within 120 min of UV light irradiation, using a catalyst concentration of 0.2 g/L.

Combined (Hybrid) photocatalysis systems

Photocatalytic membrane systems

Photocatalytic membrane systems combine photocatalysis with filtration membranes, enabling simultaneous pollutant degradation and separation. As wastewater flows through the membrane under light irradiation, contaminants degrade while the membrane acts as both a physical barrier and catalytic surface. This system can operate continuously, reducing fouling and clogging due to *in-situ* degradation. However, long-term reuse remains a challenge as persistent fouling reduces effectiveness, and high material costs limit widespread application^[61-63].

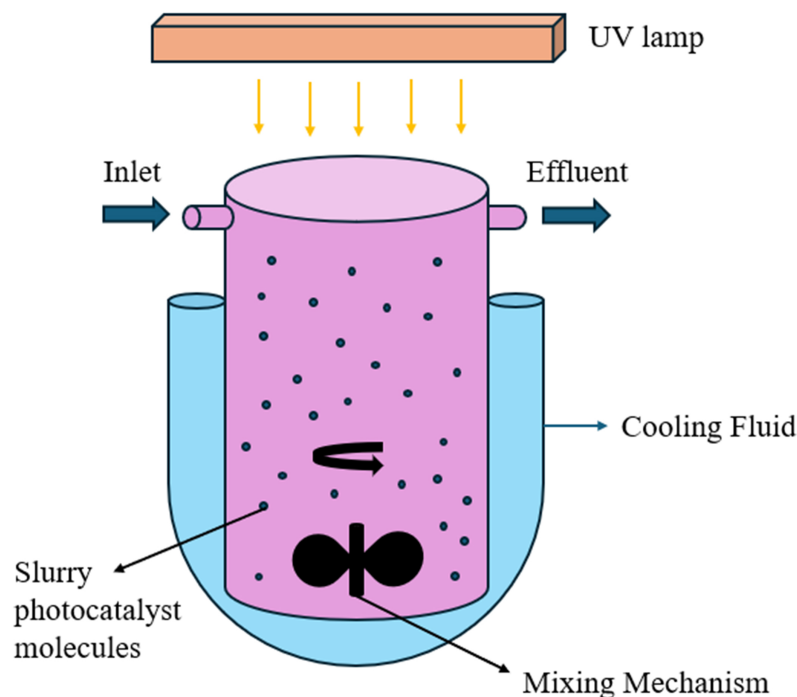


Figure 5. Schematic of a slurry photocatalyst reactor.

Espindola *et al.* utilized a photocatalytic membrane system comparing the efficiency of suspended and immobilized TiO_2 -P25 for oxytetracycline (OTC) degradation in ultrapure water (UPW) and secondary effluent water from an urban wastewater treatment plant (UWW). While the slurry system exhibited higher degradation efficiency, the immobilized system demonstrated better reusability^[64]. Nguyen *et al.* studied the degradation of diclofenac (DCF) in wastewater under visible light irradiation using a submerged photocatalytic membrane reactor (SPMR)^[65]. The DCF degradation efficiency was greater with the suspended N-doped TiO_2 (32%-42%), whereas the immobilized N-doped TiO_2 (31%) membrane resisted fouling more effectively.

PEC systems

PEC systems combine photocatalysis with electrochemical processes by applying an external electrical field to the photocatalyst, which increases its charge separation and overall performance. Upon light irradiation, the active sites of the catalyst generate electron-hole pairs, while the applied electric field assists in the transfer of electrons, thus boosting pollutant degradation. This approach reduces electron-hole recombination rate, improves efficiency, and can be applied to both gaseous and liquid matrices. However, PEC systems come at a high cost due to their complex design and reliance on external energy supply. For that reason, their scalability is limited, making them economically unfeasible for treating large volumes of wastewater. Nevertheless, these systems are being explored for water splitting for hydrogen production^[66-68].

Suhadolnik *et al.* compared the efficiency of a photocatalytic (10%) and a PEC (100%) system in degrading the textile dye Reactive Red 106 in distilled and tap water^[69]. Their results showed that photoelectrocatalysis significantly improved efficiency by hindering the recombination of electron-hole pairs. They also found that the diffusion rate is the parameter that limits the design and implementation of a PEC system for industrial wastewater treatment applications. Meng *et al.* tried developing a three-dimensional photoelectrocatalytic reactor (3D-PER) in which over 95% of the RhB dye was degraded^[70]. It was shown

that photocatalysis is responsible for degradation reactions, while electrocatalysis contributes to the mineralization of degradation products and by-products. In an effort to minimize the energy needed for the PEC system, Boschetti *et al.* developed a solar PEC reactor for the degradation of pharmaceutical pollutants^[71]. The system achieved an 84% removal efficiency, underscoring its potential for industrial-scale wastewater treatment.

PHOTOCATALYTIC REACTORS

Since conventional wastewater treatment methods seem inadequate to manage the nature of ECs, photocatalysis has piqued the interest of both scientific and engineering communities seeking sustainable waste management solutions. Photocatalysis is considered a cost-efficient, eco-friendly, and widely applicable method^[72]. Although a variety of photocatalytic reactors have been developed for experimental purposes, their adaptation for real-world industrial use - particularly for treating large volumes of wastewater at a relatively low cost - remains a major challenge^[73]. Effective reactor design is critical for maximum efficiency, which includes ensuring proper mixing of the photocatalyst and wastewater, achieving uniform light distribution, and optimizing photocatalyst utilization^[74,75].

Light source type and position

Photocatalytic reactors can utilize either natural (sunlight) or artificial light (lamps). Solar light, being cost-free, is often preferred for industrial applications, although its use is limited to daylight hours and the intensity is variable. Solar reactors can be categorized as either non-concentrated or concentrated, with the latter offering greater efficiency at the expense of increased cost^[76,77].

Artificial UV light sources provide more consistent and controllable irradiation and thus offer greater efficiency. However, they are expensive. Common UV light lamps include low-, medium-, and high-pressure mercury lamps, which have relatively short lifespans, high energy consumption, and pose environmental risks after disposal. Due to their longevity and durability, UV-LEDs are increasingly favored. Based on the position of the light source, photocatalytic reactors can be divided into three types: those with internal light sources, those using external irradiation, and those employing light transmitters to direct the radiation^[76].

Reactor processing methods

Batch photocatalytic reactors

In batch reactors, photocatalyst and wastewater are mixed without continuous flow, with stirring to ensure uniform contact. After the reaction, residual wastewater, by-products, and catalyst particles are removed^[78]. These reactors are simple, affordable, and easy to operate but unsuitable for large-scale applications due to the lack of continuous flow^[79,80]. Balarak and Kord Mostafapour used a batch reactor to optimize AMX degradation with NiO nanostructures under UV light^[81]. This setup enabled precise control of experimental parameters and reproducibility, achieving 96% degradation efficiency. They also found that increasing UV exposure time enhanced the degradation rate. Krishnan *et al.* used a batch reactor to study (TiO₂)-based photocatalytic degradation of various dyes under different conditions (catalyst dosage, light source, aeration)^[82]. Aeration improved degradation efficiency by ~15% under sunlight and ~20% under UV light, with nearly 100% degradation under UV with aeration. The reactor's simple design further contributed to its cost-effectiveness and user-friendliness.

Continuous photocatalytic reactors

Continuous photocatalytic reactors are designed for large-scale applications and are divided into Continuous Stirred Tank Reactors (CSTRs) and Plug Flow Reactors (PFRs). In CSTRs, the initial reaction

conditions are typically transient and unstable but become stable after a short operational period^[83]. Given their ability to provide continuous treatment and scalability, Yang *et al.* studied the degradation of MB using a floating photocatalyst (expanded polystyrene EPS-TiO₂) in a CSTR^[84]. They compared the degradation kinetics with those of a batch system and found that the CSTR had a higher degradation rate constant ($k = 0.0126\text{--}0.0172/\text{min}$) compared to the batch system ($k = 0.0113/\text{min}$), particularly when the wastewater flow rate was low to moderate. Tang *et al.* achieved the degradation of reactive black 5 dye using TiO₂/UV in an annular photoreactor^[85]. Ma *et al.* developed a PRF-based reactor utilizing an anaerobic process for hospital wastewater (HWW) treatment^[86]. This system demonstrated operational stability and resilience under challenging conditions over a two-year period, achieving reductions of 85%–90% and 95%–97% in BOD and COD, respectively.

Mechanics

Bed photocatalytic reactors

Recent studies have focused on enhancing the stability of immobilized photocatalysts via physical or chemical bonding, leading to the development of bed reactors. These systems offer lower mass transfer efficiency than suspended ones, making performance highly dependent on catalyst bed surface area^[87]. To address this, various bed reactor designs have emerged, with Fixed, Packed, and Fluidized bed reactors being the most common^[56,88,89]. Yusuf *et al.* used a fixed-bed photocatalytic reactor [Figure 6] to DCFA by TiO₂/β-Bi₂O₃ (TB) under UV-LED irradiation^[56]. TB was immobilized onto borosilicate beads and the results showcased the potential for refining and optimizing large-scale fixed-bed photoreactors for wastewater treatment applications. The research reported that the degradation rate constant, k , was 0.0071 at the beginning of the treatment and increased to 0.0085 after 2 years, indicating sustained catalytic activity over time. Wang *et al.* also used a fixed-bed system to investigate the photocatalytic degradation of RhB using BiFeO₃/3DOM-TiO₂-x^[90]. In addition to achieving excellent degradation efficiency (89.2%) with the synthesized catalyst, the study provided valuable insights into the kinetics of RhB degradation in a fixed-bed reactor system.

Jaiswal *et al.* explored the use of a packed-bed system for the photocatalytic degradation of p-cresol under UV light^[89]. The degradation efficiency was 98.43% at an initial concentration of 700 mg/L after 120 h [Figure 7].

Thin-film photocatalytic reactors

Thin-film reactors, suitable for lab-scale applications (50–500 mL), efficiently degrade concentrated solutions due to the minimal light penetration depth required. These systems employ an inclined flat substrate coated with a photocatalyst, enabling gravity-driven or reverse wastewater flow. Precise reaction control is achieved via self-priming pumps that mix air and fluid, enhancing distribution. The thin-film design ensures optimal light exposure and catalytic contact^[76,91]. Kahveci *et al.* synthesized unary ZnO, CuO, and CdO, as well as a ternary ZnO-CuO-CdO composite, as sunlight-driven photocatalysts for use in thin-film reactors to degrade MB^[92]. The ternary ZnO-CuO-CdO composite showed superior performance, achieving 70% degradation in 20 min.

Membrane photocatalytic reactors

Photocatalytic membrane reactors are divided into three types: (1) slurry-based systems with separate filtration; (2) integrated membranes for catalyst retention; and (3) reactors with immobilized photocatalysts, which are increasingly adopted, with some already commercially available^[93,94]. Despite their advantages, challenges include light scattering, structural complexity, high costs, and membrane fouling^[93,94]. Recent advances, such as photocatalytic ultrafiltration membrane reactors, show promising potential^[95]. Golshenas

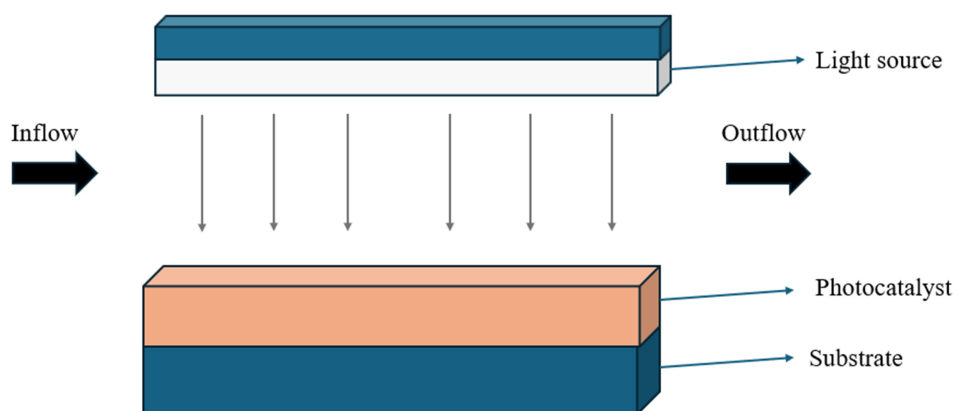


Figure 6. Simplified schematic representation of a flat-plate Fixed Bed Photoreactor.

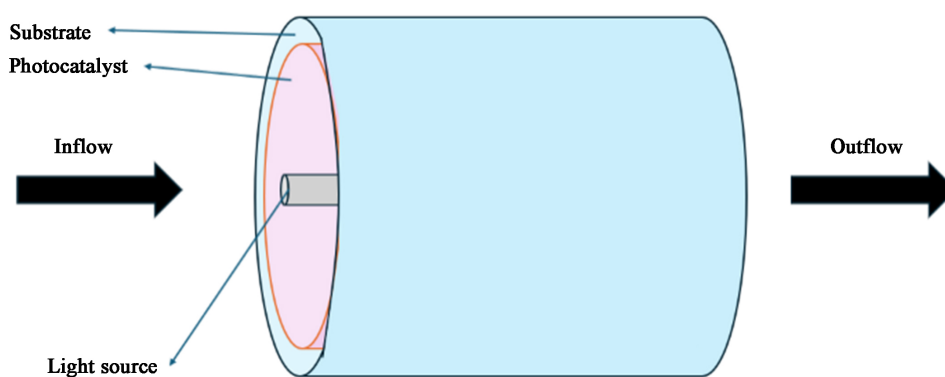


Figure 7. Simplified schematic representation of an annular Packed-Bed Photoreactor.

et al. developed a $\text{TiO}_2/\gamma\text{-Al}_2\text{O}_3$ -modified ceramic membrane for synthetic oily wastewater treatment under UV irradiation, achieving a high degradation efficiency of 90%, with industrial-scale potential^[96]. Similarly, Deepracha *et al.* fabricated a ceramic-based membrane by depositing TiO_2 on the macroporous ($3\ \mu\text{m}$) side of an asymmetric Al_2O_3 membrane combined with smectite, achieving the degradation of MB and phenol under UV light, demonstrating the potential for use in industrial continuous-flow reactors^[97]. Goma *et al.* designed a SPMR featuring a superhydrophilic ZnO NP-coated layer for simultaneous oil removal and pollutant degradation, under LED-UV light illumination^[98]. The oil removal efficiency was approximately 99%, while MB degradation was 86%.

Cascade photocatalytic reactors

Cascade reactors are not a distinct class of photocatalytic reactors but rather a configuration that combines multiple types in a sequential design where effluent undergoes progressive treatment as it flows from one stage to the next^[91]. Kubiak and Cegłowski developed a cascade continuous-flow photoreactor for the photocatalytic degradation of sulfamethoxazole (SMX) in HWW^[99]. By integrating a carbon sponge-based TiO_2 photocatalyst with a cascade system, they achieved 80% degradation efficiency, reduced energy consumption, and demonstrated potential for industrial-scale wastewater treatment in real-world applications.

Closed-loop step photocatalytic reactor

The closed-loop step photocatalytic reactor recirculates wastewater for continuous photodegradation, minimizing catalyst loss and energy use. The system uses specific light sources at various wavelengths or intensities to drive the photoreactions at each stage^[91]. Zeghioud *et al.* utilized a pilot-scale closed-loop step photocatalytic reactor to investigate the degradation of flumequine (FLU), oxolinic acid (OA), and nalidixic acid (NA)^[100]. Using TiO₂ impregnated on cellulosic paper and activated by UV light, they found that the photocatalytic rates were highest in mono-compound systems, followed by the ternary and then binary mixtures (attributed to competitive adsorption of antibiotics on the catalyst's active sites). Buehler *et al.* developed a solar-powered, closed-loop laundry facility (LaundReCycle) for laundry wastewater reuse^[101]. Operated over five weeks, the system recovered 69% of washing machine effluent and achieved 92% COD removal per cycle. Modeled data showed that 80% of the energy was internally reused, with 30% overall energy self-sufficiency. However, further optimization is needed to meet hygiene standards.

Micro-photocatalytic reactors

Micro-photocatalytic reactors employ photocatalysis at the microscale to accelerate chemical reactions under light exposure. These reactors operate at dimensions ranging from micrometers to millimeters, enhancing the surface-to-volume ratio and improving both light absorption and mass transfer efficiency^[102]. Their main advantages include shorter reaction times and the integration of microfluidic systems, where fluids flow through narrow passageways, enabling efficient mixing and uniform exposure to both the photocatalyst and the light source^[103].

Two common types of micro-photocatalytic reactors are microchannel reactors and microcapillary tube reactors, both of which can be integrated into compact systems^[104,105]. Microcapillary reactors use extremely small tubes for wastewater transport, offering a higher surface-to-volume ratio and a compact design, though scalability is limited. Moreira and Puma used helical microcapillary film (MCF) photoreactors for the degradation of pharmaceuticals in water by UV/H₂O₂^[106]. The helical design enhanced mixing, improving degradation efficiency from 4.4% to 37.9%. Hakki and Allahyari compared the degradation of methyl orange (MO) by a microcapillary photoreactor, a conventional batch photoreactor, and a tubular flow photoreactor^[107]. All systems were coated with CuPc-Bi₂O₃-ZnO and operated under visible LED light. The microcapillary reactor achieved the highest degradation efficiency (90.83%), followed by the tubular flow photoreactor (65.33%) and the batch photoreactor (58.6%). Their study also found that increasing the tube diameter while decreasing its length further improved degradation performance.

Microchannel reactors, with immobilized photocatalytic NPs in multiple channels, offer enhanced mass transfer, design flexibility, and suitability for large-scale, multi-step reactions^[108]. Yusuf *et al.* proposed a computational fluid dynamics (CFD) model for the photocatalytic degradation of 4-nitrophenol using immobilized N-TiO₂/rGO in a continuous-flow microchannel reactor with nine parallel rectangular microchannels^[109]. The degradation rate of 4-nitrophenol was observed to be proportional to the C_{eq} , allowing for straightforward estimation of rate constants. Jia *et al.* developed a spiral microchannel photocatalytic reactor using suspended TiO₂ to degrade OTC, achieving a 99.33% degradation efficiency under optimal conditions (UV-4, flow rate 1.966 mL/min, initial OTC concentration of 20 mg/L, TiO₂ dosage of 1 g/L)^[110].

Other types of photocatalytic reactors

Various other types of photocatalytic reactors exist, including hybrid designs that combine multiple configurations, such as flat-plate, spinning disk, rotating, Taylor vortex, optical fiber, biofilm, and coupled electrochemical reactors. Among them, spinning disk and rotating photocatalytic reactors are notable, as

they are mainly used for large-scale wastewater treatment^[111].

Spinning disk reactors offer high efficiency; however, scaling them up to handle massive amounts of wastewater is quite challenging. As a result, they are generally more suitable for medium-scale systems^[112]. Fallahizadeh *et al.* developed a thin-film spinning disk photocatalytic reactor coated with a visible light-activated $\text{Fe}_3\text{O}_4@\text{SiO}_2\text{-NH}_2/\text{CuO}/\text{ZnO}$ composite for the degradation of AMX^[113]. Under optimal conditions (60 min irradiation, 350 rpm, 0.9 L/min flow, pH 5, 20 mg/L AMX), the system achieved a high degradation efficiency of 98.7%, and over 69.95% COD and 61.2% TOC were also removed. Ghasemi *et al.* reported the successful degradation of MB by two novel 3D-printed components combined with UV-illuminated glass discs coated with TiO_2 ^[114]. Under optimal conditions (pH of 6.05, disc rotation speed of 22.35 rpm, initial dye concentration of 3.15×10^{-5} M, residence time of 7.98 h, and the number of NP layers set at 3.99), the system achieved a 96.63% removal rate.

In contrast, Rotating Photocatalytic Reactors utilize a different rotating element (drum or cylinder), which is coated with photocatalytic material. Due to their three-dimensional design, these reactors offer a larger surface area^[115], making them more suitable for large-scale applications. However, their efficiency can be limited by fouling and maintenance challenges^[73].

Energy and environmental costs of photocatalytic reactor systems

Photocatalytic wastewater treatment faces significant scale-up challenges, primarily due to the high costs and energy demands associated with light sources, photocatalysts, and photoreactors^[32]. These systems often require specialized materials with high UV transmittance and complex designs to ensure uniform light distribution and effective interaction between light, catalyst, and pollutants^[77,84,88]. Large-scale reactors also demand extensive surface areas or advanced configurations (e.g., thin-film or immobilized systems), which significantly increase both capital and maintenance expenses^[60,78]. While costs vary depending on the specific application and treatment objectives, a common limitation remains: the need for a sustainable, low-cost, efficient, and reliable light source to drive the system^[73,87].

Light sources play a critical role in both treatment performance and operational cost. Artificial UV light offers stable and controllable intensity but requires high energy input, whereas natural sunlight is free and renewable but fluctuates with weather conditions, location, and time of day, reducing reliability in outdoor systems^[34,57,71]. To overcome this, reactor designs can incorporate solar concentrators, light-storage technologies, or photocatalysts that remain active under diffuse or low-intensity light. Furthermore, optimizing operational parameters and designing photocatalytic systems that simultaneously generate energy, such as H_2 production or photoelectrochemical elements (electricity production), can indirectly lower both sustainability and energy costs^[37,45,58,59,71]. Ultimately, the ideal photoreactor for large-scale wastewater treatment must balance energy efficiency, cost-effectiveness, and consistent operational performance^[91].

REMOVAL OF COMMON AND EMERGING POLLUTANTS

While WWTPs are highly effective in reducing some common contaminants, the majority of common, newly emerging, and POPs^[5] often make their way through, bioaccumulate, and disrupt the environment, also posing a health hazard for human health. These contaminants originate from various sources, including urban (municipal, hospital) sewage, industrial wastewater (e.g., textile, tannery, pharmaceutical, petrochemical), and agricultural runoff. The nature of these organic pollutants spans over a range of categories.

Inorganic pollutants

The categories of inorganic pollutants identified as wastewater contaminants include acids, typically released through industrial effluents (e.g., H_2SO_4 , HNO_3), bases, primarily generated by the food processing industry and municipal sewage (e.g., NH_3), and chemical waste/heavy metals (HMs), which end up in wastewater via various industrial processes and agricultural activities^[116]. Among these, HMs are considered the most toxic inorganic compounds, posing significant threats to living organisms, particularly at high concentrations, as they tend to bioaccumulate through the food chain and can lead to mortality^[117]. Photocatalysis has emerged as an efficient method for removing HM ions from wastewater. This process works by reducing/oxidizing metal ions to lower/higher valence states or to zero-valence forms, thereby rendering them insoluble in water. During photocatalysis, ROS generated by the photocatalyst upon photon absorption facilitate these redox transformations. This approach offers the following benefits: minimal production of hazardous by-products and reduced processing time^[118,119] [Table 1].

Ma *et al.* employed a Z-scheme photocatalyst system $\text{gC}_3\text{N}_4\text{-rGO-TiO}_2$ for $\text{NH}_3\text{-N}$ removal from coking wastewater, achieving over 90% efficiency across six continuous cycles^[6].

Chen *et al.* synthesized a conjugated microporous polymer (CMP), designated TT-TPP, to selectively remove uranium (VI) from wastewater under visible light activation. Their results demonstrated removal efficiencies of over 89.9% in a 3 M NaNO_3 solution and 97.6% in simulated radioactive wastewater^[140].

Organic pollutants

Photocatalysis has emerged as an eco-friendly and highly efficient method for degrading diverse organic pollutants in wastewater, including dyes, petrochemicals, phenolics, fluorinated compounds, microplastics, pesticides, and pharmaceuticals. Dyes from textile and food industries reduce oxygen levels, block light, and bioaccumulate, with compounds like MB and RhB effectively degraded by photocatalysis^[141]. Petrochemical pollutants such as benzene, xylene, and PAHs, released from refining and plastic production, are toxic and carcinogenic but can be photocatalytically removed^[142,143]. Phenolics (e.g., chlorophenols, bisphenols) from oil, plastics, and pharma industries pose serious ecological and health threats; photocatalysis efficiently degrades them^[144]. Micro- and nanoplastics from consumer goods persist in water bodies and organisms; conventional methods fail, but photocatalysis offers a promising route^[145]. Pesticides and related agrochemicals contaminate ecosystems and foster resistance; photocatalysis has demonstrated effective removal capabilities in such cases^[146]. Pharmaceuticals, including antibiotics and hormones, remain after tertiary treatment, disrupting endocrine systems and contributing to resistance. Their complete degradation via photocatalysis is essential^[147-149]. Several examples of photocatalytic degradation of various organic pollutants are presented in Table 2.

However, concerns remain regarding the safety of the treated effluent^[147,176]. More specifically, incomplete mineralization of target compounds can lead to the formation of intermediate by-products, some of which may be more toxic than the original pollutants^[148,153,178]. These degradation products, such as short-chain organic acids, aldehydes, or nitrosamines, require thorough identification and assessment^[177]. Additionally, in slurry systems, the potential release of catalyst NPs poses a risk of nanotoxicity to aquatic life^[50]. To address these problems, treated effluents should undergo chemical analysis and ecotoxicity tests^[175,191]. Additionally, incorporating post-treatment steps, such as activated carbon filtration or biological polishing, or integrating complementary treatment methods (as discussed in Section “COMBINED TECHNOLOGIES”) can further improve safety. It is essential that the final effluent complies with regulatory standards for toxicity and contaminant levels. Thus, a comprehensive safety evaluation is critical before discharging photocatalytically treated water into the environment^[191].

Table 1. Photocatalytic removal of inorganic and radioactive [uranium (VI)] pollutants

Contaminant	Photocatalyst	Light source	Reusability	Max. efficiency	Ref.
Cr (VI)	ZFO and MFO	UV-vis light irradiation, 300-W Xe lamp	3 h cycles	99% (MFO-6-ZFO, 3 h)	[120]
	30% MnFe ₂ O ₄ /g-C ₃ N ₄ /H ₂ O ₂	350-W Xenon lamp	5 cycles	100%, 1 min	[121]
	WS ₂ /PANI nanocomposite	Xenon arc lamp	Up to 4 cycles	99%, 120 min	[122]
Cu (II)	TiO ₂ -Ni-NiO Schottky-heterojunction	Visible light (300-W xenon lamp)	5 cycles (< 48%)	86.7 %, 1 h	[123]
Hg (II)	Mesoporous 3% CuO/ZnO	Visible light (300-W xenon lamp)	5 cycles (no significant decline)	100% in 60 min	[124]
Cd (II)	Bentonite/TiO ₂ and Bentonite/ZnO	UV-A lamp	-	~70% (B/TiO ₂), ~60% (B/ZnO)	[125]
Pb (II)	TiO ₂ NPs	UV light irradiation	-	82.53% in 12 h	[126]
As (III), Cr (VI)	HCS@Fe ₂ O ₃	100W xenon lamp	5 cycles	100% [Cr (II)], 70% [As (III)], 120 min	[127]
Cu (II), Ag (I), Pb (II)	ZnO rod-shape particles	UV light irradiation	-	> 85% in 1 h	[128]
Cd (II), Pb (II)	CS/Ag thin films	Natural sunlight	-	89% [Cd (II)], 88% [Pb (II)]	[129]
U (VI)	TiO ₂ /PDA@Fe ₃ O ₄	175 W UV high-pressure Hg lamp	6 cycles	100%-83.5%, in 60 min	[130]
	ZnFe ₂ O ₄ /g-C ₃ N ₄ S-scheme	Visible LED light irradiation	5 cycles	94.62%-90%	[131]
	ZnFe ₂ O ₄ rods	Visible light (300-W xenon lamp)	-	> 95% in 40 min	[132]
	MoS ₂ /P-g-C ₃ N ₄ nanocomposites	Visible light (300-W xenon lamp)	-	99.75% in 60 min	[133]
	Mesoporous g-C ₃ N ₄	Visible light (300-W xenon lamp)	5 cycles	100% in 20 min	[134]
	Defective-enriched K ₃ PW ₁₂ O ₄₀ @WS ₂ heterojunction	Simulated sunlight (300 W Xe lamp)	4 cycles	95.6% (60 min)	[135]
	Z-Scheme heterojunction Cu ₂ (OH) ₃ F/Bi ₂ WO ₆	Simulated sunlight (300 W Xe lamp)	5 cycles	90.9%	[136]
	CdS _H /CdS _C @PB with homo/heterojunction	Visible light (300 W Hg lamp)	8 cycles	98.5% (60 min)	[137]
	CdS@NiCr-LDH Z-scheme heterojunction	25 W visible LED light	3 cycles	2,246.14 mg/g of U (VI)	[138]
	UPC-H4a	Simulated sunlight (300 W Xe lamp)	5 cycles	98.18% simulated solution, 66,14% real wastewater (120 min)	[139]

ZFO: ZnFe₂O₄; MFO: MnFe₂O₄; PANI: polyaniline; NPs: nanoparticles; CS: chitosan; LED: light-emitting diode.

Biological pollutants

Disinfection represents a crucial final step in wastewater treatment before its release into the environment and re-entry into the water cycle. Conventional WWTPs typically use chlorination, and less commonly ozonation or UV irradiation, to inactivate various pathogens^[191]. However, these methods are not

Table 2. Photocatalytic degradation of organic pollutants

Type	Contaminant	Photocatalyst	Light source	Reusability	Max. efficiency	Ref.
Microplastics	Microplastics	ZnO NPs	UV light lamp	-	-	[145]
	High-density polyethylene (HDPE)	N-TiO ₂ semiconductor	Visible light (400-800 nm)	-	6.40% in 18 h	[150]
	Polypropylene microplastics	ZnO NPs	Solar light	-	Degradation within 24 h	[151]
	PS and PET microplastics	Fe ₂ O ₃ (FeO) microparticles	NIR light (980 nm)	-	97%-98% in 80 min	[152]
	Low-density polyethylene (LDPE), polypropylene (PP), and polyamide (PA)	CuO/BiVO ₄ nanocomposites	Visible light (8 h/day for 14 days)	-	100% with more H ₂ O ₂ and longer contact time	[153]
	Poly(lactic acid) (PLA)	C ₃ N ₄ /Bi ₁₂ O ₁₇ C ₁₂ (CN/BOC) on a polyacrylonitrile (PAN) membrane (CN/BOC/PAN)	Visible light irradiation	5 cycles	Maximum product conc. At 12 h	[154]
PFAS	PFOA	FeOCl/(Bi-MOF-BiOCl) ₁₀₀ with oxygen defects	UV light (240 min)	-	> 99.9% PFOA in 30 min and 64.3% defluorination efficiency	[155]
		MIL-125-NH ₂	UV light	3 cycles	> 98.9% in 24 h	[156]
	Perfluorononanoic acid (PFNA)		UV light (365 nm)	-	100% in 22 h	[157]
Phenolic compounds	Phenolic compounds	gAu/RGO nanocomposite	Visible light irradiation	6-7 cycles	95.78% in 130 min	[158]
		Mesoporous TiO ₂ NPs	UVA lamps	5 times	100% in 140 min	[159]
	Phenol	LaVO ₄ /MCM-48 nanocomposite	Visible light	6 cycles	99.9% in 3 h	[160]
		CeO ₂ NPs synthesized at dif. temp.	UV lamp	3 cycles	62% in 5 h	[144]
		TiO ₂ /SR and ZnO/SR	Visible light	YES	87% (TiO ₂ /SR), 70% (ZnO/SR)	[161]
Petrochemical wastewater	Petrochemical wastewater	Co-TiO ₂ /zeolite and K ₂ S ₂ O ₈	UV light (254 nm)	YES	93.40%	[142]
	Petroleum wastewater	g-C ₃ N ₄ /Ce-ZnO	Simulated and direct sunlight radiation	-	88% simulated irradiation, 52% direct sunlight	[162]
	Crude oil wastewater	MIL-101(Fe)	UV light irradiation	> 5 times	94.73% in 30 min	[163]
	Polycyclic aromatic hydrocarbons (PAHs)	NiO NPs	UV and VIS light for 300 min	-	70% (UV light), 64% (sunlight)	[164]
		N-TiO ₂ /ASC-PVP	Visible light	4 cycles	98.6% in 120min	[165]
	2,6-dichlorophenol (2,6-DCP)	Fe/Zn@biochar composite	Parabolic solar collector system	-	> 90% in 4 h	[143]
Dyes	MB	FeWO ₄ @N-TiO ₂	Visible light ($\lambda \geq 420$ nm)	3 times	77% in 2 h	[141]
	Acid violet 7 dye (AV7)	ZnS-SnO ₂ (60ZS) heterostructure/nanocomposite	Visible light with ~3% UV radiation	5 cycles	94.71% in 60 min	[166]
	Tartrazine Y5	Carbon-containing Cu-based material (Cu@C)	CPC, artificial solar light and sunlight	-	100% for solar CPC in 10 h	[167]
	MB	SiO ₂ @WO ₃ @Fe ₃ O ₄	Visible light irradiation	4 cycles	> 90% in 120 min	[168]

	CR		BiOCl–ZnFe ₂ O ₄ /CNTs	Natural sunlight	4 cycles	95.27% in 2 h	[169]
Herbicide	Pendimethalin		BiOCl–ZnFe ₂ O ₄ /CNTs	Natural sunlight	4 cycles	88.6% in 2 h	[169]
Fungicide	Imazalil		Open-cell ceramic foams covered with TiO ₂	Natural sunlight and UVA (lab)	5 cycles	95% in 30 min	[146]
Pesticide	2,4-dichlorophenoxyacetic acid (2,4D)		MI TiO ₂ /2,4D	UV light irradiation	5 cycles	74% in 240 min	[170]
Insecticides	Thiamethoxam, imidacloprid, acetamiprid and thiacloprid		TiO ₂ with Na ₂ S ₂ O ₈	Natural sunlight	YES	100% (thiamethoxam), ~99.7% (imidacloprid), ~97% (acetamiprid), ~99.97% (thiacloprid)	[171]
Pharmaceuticals	Antibiotics	TC	PC/GO-CTS (protonated carbon/graphene oxide-Cu ₃ SnS ₄)	UV light	-	95.6% in 45 min	[172]
		Spiramycin (SPY)	ZnO	UV light	-	95%-99% in 80 min	[173]
		Ofloxacin (OFL) and SMX	Bi ₂₄ O ₃₁ Br ₁₀ (BOB)	Visible light irradiation	5 cycles	OFL > 95.5% SMX 57%, in 2 h	[174]
	Psychiatric drugs	Amisulpride	g-C ₃ N ₄	UVA light radiation	-	86% in water (60 min)	[175]
		Sertraline hydrochloride (SERT)	ZnO-NPs	UV light irradiation	-	98.7% in 30 min	[176]
		Bupropion (BUP)	TiO ₂	UV light irradiation	-	100% in 90 min	[177]
		CBZ	C ₃ N ₄ /Bi ₁₂ O ₁₇ C ₁₂ (CN/BOC) on a PAN membrane (CN/BOC/PAN)	Visible light irradiation	5 cycles	100% in 180 min (for 19 of the 20 pharmaceuticals)	[154]
	Cytostatics	Etoposide (ETO)	TiO ₂ Degussa P25	UV light irradiation	-	40% of ETO at pH 5 and 9 in 2 h	[178]
		Kabi cytarabine	Bismuth iron oxide (BFO)	UV light irradiation	5 cycles	97.9% in 120 min	[179]
		5-fluorouracil	Ni ₃ (VO ₄) ₂ /ZnCr ₂ O ₄ Z-scheme	Visible light irradiation	6 cycles	98.9% in 200 min	[180]
	Hormones	Estriol (E3) hormone	TiO ₂ /Nd polyurethane nanofibers	UV and visible light irradiation	2 cycles	~90.2% at pH = 7, 120 min under UV	[181]
		Estrone hormone	Silica-supported g-C ₃ N ₄ /WO ₃	UV and visible light irradiation for 3 h	7 cycles	100% under UV, 96% under visible	[182]
	Lipid regulators	Gemfibrozil	Ag@mpgC ₃ N ₄	-	> 5 cycles	> 90% in 60 min	[183]
	Anti-histamines	Chlorpheniramine	XFe1.0 (Fe doped carbon material)	Solar light irradiation	2 cycles	82%-91% for XFe1.0	[184]
	Anti-inflammatories	Ketorolac tromethamine	Zn _{0.5} Cd _{0.5} S/MoS ₂ S-scheme	Natural solar light	5 cycles	92.54% in 150 min	[185]
		Ibuprofen (IBP)	Bi ₂₄ O ₃₁ Br ₁₀ (BOB)	Visible light irradiation	5 cycles	IBP > 95.5 % in 2 h	[174]
	Antivirals	Paracetamol (aka acetaminophen, APAP)	NASICON@C	Visible light irradiation	5 cycles	99.7% in 30 min	[186]
		Lopinavir (LOPI), ritonavir (RITO)	Ni-doped ZnO/SiO ₂ nanocomposites	UV light irradiation	4 times	100% of RITO in 60 min (by all) and 100% of LOPI in 30 min (by 6-Ni-ZnO/SiO ₂)	[187]
			Multiphase photocatalysts (WU and WW)	Visible light irradiation	3 cycles	95% of RITO (15 min) 95% of LOPI (60 min)	[188]

	Favipiravir (FAV)	Bi ₂₄ O ₃₁ Br ₁₀ (BOB)	Visible light irradiation	5 cycles	FAV > 95.5 % in 2 h	[174]
Beta-blockers	Metoprolol (Met), propranolol (Pro)	Biochar-doped TiO ₂	Simulated visible light for 60 min	3 times	70% (Pro) 60% (Met)	[189]
	Atenolol (AT), metoprolol (ME)	ZnO NPs/Zeolite and TiO ₂ NPs/Zeolite	UV light for 60 min	5-6 times	83.2% of AT (TiO ₂ NPs/Zeolite) and 83.1% of ME (ZnO NPs/Zeolite)	[190]

NPs: Nanoparticles; PS: polystyrene; PET: polyethylene terephthalate; NIR: near-infrared; PFOA: perfluorooctanoic acid; MB: methylene blue; CR: Congo red; TC: tetracycline; SMX: sulfamethoxazole; CBZ: carbamazepine.

always cost-effective and often fail to completely eliminate the most resistant microorganisms (bacteria, fungi, parasites, viruses, *etc.*), particularly those present in HWW^[192,193]. *Escherichia coli*, *Enterococcus*, *Pseudomonas*, *Aspergillus fumigatus*, *Candida*, *norovirus*, *sapovirus*, and *enteric adenovirus* are a few of the common pathogenic microorganisms in wastewater that can cause diarrhea, respiratory system infections, and gastrointestinal diseases in humans^[194].

A highly dangerous subcategory of biological pollutants includes antibiotic-resistant bacteria (ARB), which are found in relatively high concentrations in HWW. This comes as a result of the extensive use of antibiotics, which drives bacterial evolution toward expressing antibiotic resistance genes (ARGs) and producing antibiotic-resistant proteins (ARPs). These proteins employ various resistance mechanisms, including reduced permeability, increased efflux, target site mutation or protection, and direct antibiotic modification through hydrolysis or chemical group transfer^[195]. Furthermore, it has been proven that certain advanced treatment methods are able to inactivate ARBs even in complex wastewater matrixes^[196,197] [Table 3].

COMBINED TECHNOLOGIES

To improve photocatalysis and pollutant removal in wastewater treatment, researchers are exploring integrated approaches combining multiple technologies. Studies have merged these with photocatalysis to boost efficiency, minimize limitations, and enable energy recovery^[216,217].

The combination of photocatalysis with AOPs, such as ozonation and Fenton/Fenton-like reactions, has been extensively studied for its potential to enhance wastewater treatment efficiency. Photocatalytic ozonation offers significant advantages over individual methods, as it improves the mass transfer limitations of fixed catalysts and generates a higher concentration of reactive $\cdot\text{OH}$. Studies such as those by Xiao *et al.* demonstrated the high degradation capability of visible light-activated graphitic carbon nitride (g-C₃N₄) in a light/O₃/photocatalyst system. More specifically, using g-C₃N₄ for photocatalytic ozonation (vis/O₃/g-C₃N₄) causes the mineralization of oxalic acid (model pollutant) at a rate 95.8 times higher than the sum of photocatalytic oxidation (vis/O₂/g-C₃N₄) and ozonation alone (100% degradation in 2 and 20 min, respectively)^[218]. Rodríguez *et al.* investigated the degradation of N, N-diethyl-m-toluamide (DEET) using TiO₂-supported mullite ceramic foams and glass Raschig rings, showing that photocatalytic ozonation enhances carboxylate formation and mineralization rates with minimal interference from the wastewater matrix, resulting in a 25% increase in efficiency^[219]. The combination of photocatalysis with photo-Fenton reactions enables catalyst regeneration, higher efficiency, and operation across a broader pH range. Jiad and Abbar applied a photo-Fenton catalytic system with TiO₂,

Table 3. Photocatalytic inactivation of bacteria, fungi, parasites, viruses, phage and ARBs/ARGs

Type	Contaminant	Photocatalyst	Light source	Reusability	Max. efficiency	Ref.
Bacteria	<i>E. coli</i> and <i>S. aureus</i>	α/β -Bi ₂ O ₃ composite	LED lamp (430-800 nm)	3 cycles	99% <i>E. coli</i> and 98% <i>S. aureus</i> , in 240 min	[198]
	<i>Escherichia coli</i> , <i>Staphylococcus aureus</i> , <i>Enterococcus faecalis</i>	Pd-loaded BiFeO ₃ micro composites	Visible light	6 cycles	100% in 180 min	[199]
	<i>Pseudomonas aeruginosa</i>	TiO ₂	UVA irradiation for 60 min	-	Inactivated by 4 log units	[200]
	<i>Escherichia coli</i> and <i>Staphylococcus aureus</i>	WCF@PCN-222/Ag ₂ O-Ag	Visible light for 90 min	Outstanding reusability	99.99% (inactivated by 6 log units)	[201]
Fungi	Pathogens in UWW effluent	Gd-BiVO ₄	UVA-LED lamp (370 nm)	-	Almost completely (180 min)	[202]
	<i>Fusarium equiseti</i>	TiO ₂	UV light for 4 h/day	-	50% in 14 days	[201]
	<i>Aspergillus niger</i>	Pd-loaded BiFeO ₃ micro composites	Visible light irradiation	6 cycles	100% in 180 min	[199]
Parasites	<i>Cryptosporidium parvum</i>	Fe ²⁺ /H ₂ O ₂	Solar radiation, 4 and 6 h	-	96.32% (4 h) and 93.61% (6 h)	[202]
	<i>Giardia lamblia</i>	H ₂ O ₂	UV-LED (255/280/400 nm)	-	92% in one sample	[203]
Virus	Influenza virus	TiO ₂ NP and nanotubular surfaces	UV light irradiation λ max = 365 nm, 2 h	-	-	[204]
Phage	Human adenoviruses (HAdVs)	g-C ₃ N ₄ /WO ₃ /biochar	6-h visible light irradiation	-	5-log complete inactivation	[205]
	Viral surrogates (phage MS2)	g-C ₃ N ₄ @COF	60 min visible light irradiation	4 cycles	6 logs of MS2 removal	[206]
	Bacteriophage MS2	rGO-supported g-C ₃ N ₄ (7.5% GCN)	$\lambda > 400$ nm and $\lambda > 305$ nm	-	3.20 log ($\lambda > 400$ nm) and 3.27 log ($\lambda > 305$ nm), in 2 h	[207]
	PhiX174 bacteriophage	Cu-doped TiO ₂ nanorods	Visible light (150 W Xe lamp)	5 cycles	Inactivation rate 0.42 log inactivation/min	[208]
	Bacteriophage f2	Cu-TiO ₂ nanofibers	Visible light (400 nm)	4 cycles	100% in 2 h	[209]
	Lactococcus phages	Photocatalytic paint (with carbon-doped anatase TiO ₂) wall photoreactor coating	Visible light (360-720 nm)	-	100% in 1.5-5 h (for 8 phages)	[210]
ARBs/ARGs	<i>Shigella flexneri</i> HL	60%-BiVO ₄ /EAQ Z-heterojunction	Simulated sunlight (500-W xenon lamp)	YES	100% inactivation in 150 min	[211]
	Methicillin-resistant <i>Staphylococcus aureus</i> (MRSA)	Cu-BiOCl with nanosheets assembled into spheres	500 W Xenon lamp ($\lambda \geq 290$ nm)	-	3.5 log units of removal	[212]
	<i>E. coli</i> DH5 α with blaTEM-1 and tetA in plasmid pWH1266 and its plasmid DNA carrying eARG	Urea-based g-C ₃ N ₄	Simulated solar irradiation	-	6.2 log units reduction (100%, in water) and 4.3 log units reduction of ARB (real wastewater)	[213]
	tetA and ampC ARGs in ARBs	Ag/TiO ₂ /graphene oxide (GO)	Xe light irradiation with a 420 nm cut-off	-	100% removal efficiency of both ARGs under optimal conditions	[214]
	<i>Shigella flexneri</i> HL	MWCNT/M-BiVO ₄ /T-BiVO ₄	Simulated solar irradiation	4 cycles	100% inactivation by C/BVO-1 in 180 min	[215]

ARBs: Antibiotic-resistant bacterias; ARGs: antibiotic resistance genes; LED: light-emitting diode; UWW: urban wastewater; NP: nanoparticle.

achieving significant COD reduction in petroleum refinery wastewater (68.122% and 91.26% removal efficiency for photocatalysis and the combined process, respectively, showcasing an increase of ~23% in removal rate)^[220]. Xu *et al.* developed a photocatalytic fuel cell (PFC) system integrating electro-Fenton (WO_3/W photoanode) and $\text{Fe@Fe}_2\text{O}_3/\text{carbon}$ cathode, demonstrating enhanced organic pollutant degradation alongside simultaneous energy generation. This system achieved 91.6% degradation, significantly outperforming the individual methods (77.2% for EF and 68.3% for PC). The system's performance was highly pH-dependent: optimal degradation (91.6%) occurred at pH 3, while efficiency declined at both lower (82.7% at pH 1.5-3) and higher pH values (71.8% at pH 4.5)^[221].

The integration of microalgae systems with photocatalysis enhances pollutant degradation by producing oxygen, promoting ROS formation, and preventing catalyst fouling. Additionally, they absorb nutrients, degrade pathogens, and improve wastewater treatment efficiency^[222]. Li *et al.* demonstrated a sequential system where photocatalysis degraded antibiotics, while microalgae further reduced toxicity. However, the effectiveness varied depending on the microalgae species used. In their study, *C. pyrenoidosa* achieved a 98% higher degradation efficiency of photocatalysis by-products compared to *S. obliquus*^[223]. Similarly, Lu *et al.* reported improved enrofloxacin degradation efficiency (rising from 57% to 64%) in a two-step system combining photocatalysis with microalgae treatment^[224]. de Souza *et al.* also applied a sequential photocatalysis-microalgae system to treat Cr(VI)-contaminated wastewater, achieving a 7%-20% higher degradation efficiency compared to either method used individually^[225]. Another promising hybrid method is sonophotocatalysis, where ultrasound waves enhance photocatalysis by generating ROS, increasing mass transfer, and improving catalyst regeneration^[226]. Schieppati *et al.* showed that sonophotocatalysis degraded herbicide Isoproturon faster than photocatalysis alone, achieving complete degradation within 60 min, compared to 240 min with photocatalysis alone^[227]. Karim and Shrivastav designed a multi-frequency reactor for antibiotic degradation and found that simultaneous application of ultrasound and visible light achieved 44% degradation efficiency in 90 min, compared to 41.4% with sonocatalysis^[228]. However, the high cost of sonophotocatalysis remains a challenge. To address this, Khalegh and Qaderi developed a cost-effective design for textile wastewater treatment, calculating that under optimal conditions, complete removal of 1 mg of MB in 13.695 min would cost only 0.001¢^[229]. Constructed wetlands (CWs) coupled with photocatalysis offer another sustainable treatment method^[230]. Nguyen *et al.* demonstrated that combining CWs with TiO_2 -based photocatalysis increased organic matter degradation to levels compliant with THM standards if chlorination was applied to the treated water^[231]. Chen *et al.* compared three CW-photocatalysis configurations for removing ARGs, finding that CWs effectively removed intracellular ARGs, while photocatalysis targeted extracellular ARGs. When combined, the system achieved a 99.8% removal efficiency, compared to only 50%-60% with each method alone^[230].

Dindaş *et al.* investigated the treatment of pharmaceutical wastewater using a combination of electrocoagulation (EC), electro-Fenton (EF), and photocatalytic oxidation processes. Their results highlighted the main role of photocatalysis, especially when paired with EF, reaching a 64% removal rate compared to 26.84% for EF alone and 39.9% for the combination of photocatalysis and EC^[232]. Similarly, Aldana *et al.* integrated membrane filtration, activated sludge, and solar photocatalysis, and compared various membranes for the treatment of table olive processing wastewater, achieving 60%-90% pollutant removal^[233]. Kusworo *et al.* fabricated a UV-light-driven photocatalytic nanohybrid membrane ($\text{PVDF/GO-NiFe@SiO}_2$), coupled with bentonite adsorption and an ozonation process, for effective and sustainable textile wastewater treatment, increasing removal efficiency from 55.11% to 97.22%^[234]. Majumder *et al.* employed a multi-stage system comprising a bed-type bio-reactor sedimentation tank (MBSST), an aerated horizontal flow constructed wetland (AHFCW), and photocatalysis to treat real HWW spiked with carbamazepine (CBZ). MBSST and AHFCW in combination removed 85% of COD, 93% of TSS, 99% of

NH₃, but only 30% of CBZ. However, applying photocatalysis to the effluent from the AHFCW raised CBZ removal to 85%. Furthermore, the intermediate products (IPs) generated through photocatalysis were found to be less toxic than those formed during the earlier biological treatment stages^[235].

Overall, combined technologies integrating photocatalysis with membrane filtration, electrochemical oxidation, Fenton reactions, and biological treatments are gaining momentum in industrial wastewater remediation, as they offer synergistic advantages, such as enhanced degradation efficiency and broader pollutant removal spectra^[230,231]. However, they often involve high capital, material and maintenance costs due to complex configurations, high energy demands, and issues such as membrane fouling and catalyst deactivation^[217,233,234]. Despite these limitations, such integrated approaches can be cost-effective for treating high-strength wastewater (e.g., those from dye, pharmaceutical, or petrochemical industries), especially when solar-driven photocatalysis reduces energy consumption. Optimization of operational parameters (e.g., pH, photocatalysis duration, sequence and combination of methods, *etc.*) can further improve treatment efficiency and lower costs^[224,227,233,235]. Additionally, coupling photocatalysis with PFCs offers indirect cost savings by generating electricity during the treatment process^[221]. Although scalability remains a challenge, modular and application-specific system designs are gradually facilitating industrial adoption and offering relatively stable operation, as previously discussed^[226,229]. Several studies, such as that by Khalegh and Qaderi, have also examined the cost-effectiveness of removing MB using a photocatalytic/ultrasonic hybrid system^[229]. In summary, combined technologies offer high oxidation power, rapid reaction rates, broad-spectrum pollutant removal, and improved energy efficiency, making them promising candidates for future wastewater treatment systems^[220,222].

CONCLUSION AND FUTURE PROSPECTS

Photocatalysis presents a promising solution for wastewater treatment, offering effective degradation of pollutants with minimal chemical use and potential for solar energy integration. However, key challenges persist, including limited efficiency, catalyst instability, poor recyclability, and difficulties in scaling up from laboratory experiments to industrial applications. Future research should prioritize the development of durable and cost-effective photocatalysts, the optimization of reactor designs, and the reduction of harmful by-products. Moreover, integrating photocatalysis with other advanced treatment methods - such as AOPs, membrane filtration, absorption, biological treatment, and electrochemical methods - offers significant potential to enhance treatment efficiency, expand the range of removable contaminants, and improve scalability. Addressing these challenges will be crucial for unlocking the full potential of photocatalysis for sustainable, large-scale wastewater treatment.

DECLARATIONS

Authors' contributions

Writing - original draft, investigation: Chalatsi-Diamanti, P.

Writing - original draft and editing: Isari, E. A.; Grilla, E.

Made substantial contributions to the conception, design and review of the study: Kokkinos, P.

Supervision: Kalavrouziotis, I. K.

Availability of data and materials

Not applicable.

Financial support and sponsorship

None.

Conflicts of interest

All authors declared that there are no conflicts of interest.

Ethical approval and consent to participate

Not applicable.

Consent for publication

Not applicable.

Copyright

© The Author(s) 2025.

REFERENCES

1. Zhang, D.; Sial, M. S.; Ahmad, N.; et al. Water scarcity and sustainability in an emerging economy: a management perspective for future. *Sustainability* **2021**, *13*, 144. DOI
2. van Vliet, M. T. H.; Jones, E. R.; Flörke, M.; et al. Global water scarcity including surface water quality and expansions of clean water technologies. *Environ. Res. Lett.* **2021**, *16*, 024020. DOI
3. Morin-Crini, N.; Lichtfouse, E.; Liu, G.; et al. Worldwide cases of water pollution by emerging contaminants: a review. *Environ. Chem. Lett.* **2022**, *20*, 2311-38. DOI
4. Saravanan, A.; Senthil, K. P.; Jeevanantham, S.; et al. Effective water/wastewater treatment methodologies for toxic pollutants removal: processes and applications towards sustainable development. *Chemosphere* **2021**, *280*, 130595. DOI
5. United Nations Environment Programme. Stockholm Convention on Persistent Organic Pollutants (POPs). <https://www.pops.int/>. (accessed 28 May 2025).
6. Ma, D.; Yi, H.; Lai, C.; et al. Critical review of advanced oxidation processes in organic wastewater treatment. *Chemosphere* **2021**, *275*, 130104. DOI
7. Li, H.; Cao, Y.; Liu, P.; et al. Ammonia-nitrogen removal from water with gC₃N₄-rGO-TiO₂ Z-scheme system via photocatalytic nitrification-denitrification process. *Environ. Res.* **2022**, *205*, 112434. DOI PubMed
8. Ren, G.; Han, H.; Wang, Y.; et al. Recent advances of photocatalytic application in water treatment: a review. *Nanomaterials* **2021**, *11*, 1804. DOI PubMed PMC
9. Ajmal, A.; Majeed, I.; Malik, R. N.; Idriss, H.; Nadeem, M. A. Principles and mechanisms of photocatalytic dye degradation on TiO₂ based photocatalysts: a comparative overview. *RSC. Adv.* **2014**, *4*, 37003-26. DOI
10. Wang, H.; Zhang, L.; Chen, Z.; et al. Semiconductor heterojunction photocatalysts: design, construction, and photocatalytic performances. *Chem. Soc. Rev.* **2014**, *43*, 5234-44. DOI
11. Datta, P.; Roy, S. Recent development of photocatalytic application towards wastewater treatment. *Catal. Res.* **2023**, *3*, 1-23. DOI
12. Rahim Pouran, S.; Abdul Aziz, A. R.; Wan Daud, W. M. A. Review on the main advances in photo-fenton oxidation system for recalcitrant wastewaters. *J. Ind. Eng. Chem.* **2015**, *21*, 53-69. DOI
13. Lee, D.; Kim, M.; Danish, M.; Jo, W. State-of-the-art review on photocatalysis for efficient wastewater treatment: attractive approach in photocatalyst design and parameters affecting the photocatalytic degradation. *Catal. Commun.* **2023**, *183*, 106764. DOI
14. Ahuja, T.; Brighu, U.; Saxena, K. Recent advances in photocatalytic materials and their applications for treatment of wastewater: a review. *J. Water. Process. Eng.* **2023**, *53*, 103759. DOI
15. Jorfi, S.; Barzegar, G.; Ahmadi, M.; et al. Enhanced coagulation-photocatalytic treatment of Acid red 73 dye and real textile wastewater using UVA/synthesized MgO nanoparticles. *J. Environ. Manage.* **2016**, *177*, 111-8. DOI
16. Souza, R. P.; Freitas, T. K.; Domingues, F. S.; et al. Photocatalytic activity of TiO₂, ZnO and Nb₂O₅ applied to degradation of textile wastewater. *J. Photochem. Photobiol. A.* **2016**, *329*, 9-17. DOI
17. García-Muñoz, P.; Pliego, G.; Zazo, J. A.; et al. Treatment of hospital wastewater through the CWPO-photoassisted process catalyzed by ilmenite. *J. Environ. Chem. Eng.* **2017**, *5*, 4337-43. DOI
18. Che, W.; Luo, Y.; Deng, F.; et al. Facile solvothermal fabrication of cubic-like reduced graphene oxide/AgIn₂S₈ nanocomposites with anti-photocorrosion and high visible-light photocatalytic performance for highly-efficient treatment of nitrophenols and real pharmaceutical wastewater. *Appl. Catal. A. Gen.* **2018**, *565*, 170-80. DOI
19. Mahdizadeh, F.; Aber, S. Treatment of textile wastewater under visible LED lamps using CuO/ZnO nanoparticles immobilized on scoria rocks. *RSC. Adv.* **2015**, *5*, 75474-82. DOI
20. Ahmad, I.; Zou, Y.; Yan, J.; et al. Semiconductor photocatalysts: a critical review highlighting the various strategies to boost the photocatalytic performances for diverse applications. *Adv. Colloid. Interface. Sci.* **2023**, *311*, 102830. DOI
21. Bahadoran, A.; De Lile, J. R.; Masudy-Panah, S.; et al. Photocatalytic materials obtained from E-waste recycling: review, techniques, critique, and update. *JMMP.* **2022**, *6*, 69. DOI
22. Chen, Y.; Xu, M.; Wen, J.; et al. Selective recovery of precious metals through photocatalysis. *Nat. Sustain.* **2021**, *4*, 618-26. DOI

23. Hong, J.; Cho, K.; Presser, V.; Su, X. Recent advances in wastewater treatment using semiconductor photocatalysts. *Curr. Opin. Green. Sustain. Chem.* **2022**, *36*, 100644. [DOI](#)
24. Bai, S.; Zhang, N.; Gao, C.; Xiong, Y. Defect engineering in photocatalytic materials. *Nano. Energy*. **2018**, *53*, 296-336. [DOI](#)
25. Wang, J.; Cao, C.; Zhang, Y.; Zhang, Y.; Zhu, L. Underneath mechanisms into the super effective degradation of PFOA by BiOF nanosheets with tunable oxygen vacancies on exposed (101) facets. *Appl. Catal. B. Environ.* **2021**, *286*, 119911. [DOI](#)
26. Wu, Y.; Li, Y.; Fang, C.; Li, C. Highly efficient degradation of perfluorooctanoic acid over a MnO_x-modified oxygen-vacancy-rich In₂O₃ photocatalyst. *ChemCatChem* **2019**, *11*, 2297-303. [DOI](#)
27. Núñez-Salas, R. E.; Hernández-Ramírez, A.; Hinojosa-Reyes, L.; Guzmán-Mar, J. L.; Villanueva-Rodríguez, M.; Maya-Treviño, M. D. L. Cyanide degradation in aqueous solution by heterogeneous photocatalysis using boron-doped zinc oxide. *Catal. Today*. **2019**, *328*, 202-9. [DOI](#)
28. Aboutaleb, W. A.; El-Salamony, R. A. Effect of Fe₂O₃-CeO₂ nanocomposite synthesis method on the Congo red dye photodegradation under visible light irradiation. *Mater. Chem. Phys.* **2019**, *236*, 121724. [DOI](#)
29. Shabbir, A.; Sardar, S.; Mumtaz, A. Mechanistic investigations of emerging type-II, Z-scheme and S-scheme heterojunctions for photocatalytic applications - a review. *J. Alloys. Compd.* **2024**, *1003*, 175683. [DOI](#)
30. Abbood, N. S.; Ali, N. S.; Khader, E. H.; Majdi, H. S.; Albayati, T. M.; Saady, N. M. C. Photocatalytic degradation of cefotaxime pharmaceutical compounds onto a modified nanocatalyst. *Res. Chem. Intermed.* **2023**, *49*, 43-56. [DOI](#)
31. He, X.; Kai, T.; Ding, P. Heterojunction photocatalysts for degradation of the tetracycline antibiotic: a review. *Environ. Chem. Lett.* **2021**, *19*, 4563-601. [DOI](#) [PubMed](#) [PMC](#)
32. Morshedy, A. S.; El-Fawal, E. M.; Zaki, T.; El-Zahhar, A. A.; Alghamdi, M. M.; El Naggar, A. M. A review on heterogeneous photocatalytic materials: mechanism, perspectives, and environmental and energy sustainability applications. *Inorg. Chem. Commun.* **2024**, *163*, 112307. [DOI](#)
33. Khurram, R.; Wang, Z.; Ehsan, M. F. α-Fe₂O₃-based nanocomposites: synthesis, characterization, and photocatalytic response towards wastewater treatment. *Environ. Sci. Pollut. Res. Int.* **2021**, *28*, 17697-711. [DOI](#)
34. Kumar, A.; Khan, M.; He, J.; Lo, I. M. C. Recent developments and challenges in practical application of visible-light-driven TiO₂-based heterojunctions for PPCP degradation: a critical review. *Water. Res.* **2020**, *170*, 115356. [DOI](#) [PubMed](#)
35. Paul, T.; Das, D.; Das, B. K.; Sarkar, S.; Maiti, S.; Chattopadhyay, K. K. CsPbBrCl₂/g-C₃N₄ type II heterojunction as efficient visible range photocatalyst. *J. Hazard. Mater.* **2019**, *380*, 120855. [DOI](#)
36. Cui, H.; Dong, S.; Wang, K.; Luan, M.; Huang, T. Synthesis of a novel Type-II In₂S₃/Bi₂MoO₆ heterojunction photocatalyst: excellent photocatalytic performance and degradation mechanism for Rhodamine B. *Sep. Purif. Technol.* **2021**, *255*, 117758. [DOI](#)
37. Opoku, F.; Govender, K. K.; van Sittert, C. G. C. E.; Govender, P. P. Recent progress in the development of semiconductor-based photocatalyst materials for applications in photocatalytic water splitting and degradation of pollutants. *Adv. Sustain. Syst.* **2017**, *1*, 1700006. [DOI](#)
38. Wen, X.; Shen, C.; Fei, Z.; et al. Recent developments on AgI based heterojunction photocatalytic systems in photocatalytic application. *Chem. Eng. J.* **2020**, *383*, 123083. [DOI](#)
39. Li, J.; Chen, J.; Fang, H.; Guo, X.; Rui, Z. Plasmonic metal bridge leading Type III heterojunctions to robust Type B photothermocatalysts. *Ind. Eng. Chem. Res.* **2021**, *60*, 8420-9. [DOI](#)
40. Jiang, X.; Wang, Z.; Zhang, M.; et al. A novel direct Z-scheme heterojunction BiFeO₃/ZnFe₂O₄ photocatalyst for enhanced photocatalyst degradation activity under visible light irradiation. *J. Alloys. Compd.* **2022**, *912*, 165185. [DOI](#)
41. Luo, J.; Ning, X.; Zhan, L.; Zhou, X. Facile construction of a fascinating Z-scheme AgI/Zn₃V₂O₈ photocatalyst for the photocatalytic degradation of tetracycline under visible light irradiation. *Sep. Purif. Technol.* **2021**, *255*, 117691. [DOI](#)
42. Chen, M.; Guo, C.; Hou, S.; et al. A novel Z-scheme AgBr/P-g-C₃N₄ heterojunction photocatalyst: excellent photocatalytic performance and photocatalytic mechanism for ephedrine degradation. *Appl. Catal. B. Environ.* **2020**, *266*, 118614. [DOI](#)
43. Xu, Q.; Zhang, L.; Yu, J.; Wageh, S.; Al-Ghamdi, A. A.; Jaroniec, M. Direct Z-scheme photocatalysts: principles, synthesis, and applications. *Mater. Today*. **2018**, *21*, 1042-63. [DOI](#)
44. Beshkar, F.; Al-Nayili, A.; Amiri, O.; Salavati-Niasari, M.; Mousavi-Kamazani, M. Visible light-induced degradation of amoxicillin antibiotic by novel CuI/FePO₄ p-n heterojunction photocatalyst and photodegradation mechanism. *J. Alloys. Compd.* **2022**, *892*, 162176. [DOI](#)
45. Hasija, V.; Kumar, A.; Sudhaik, A.; et al. Step-scheme heterojunction photocatalysts for solar energy, water splitting, CO₂ conversion, and bacterial inactivation: a review. *Environ. Chem. Lett.* **2021**, *19*, 2941-66. [DOI](#)
46. Fan, H.; Zhou, H.; Li, W.; Gu, S.; Zhou, G. Facile fabrication of 2D/2D step-scheme In₂S₃/Bi₂O₂CO₃ heterojunction towards enhanced photocatalytic activity. *Appl. Surf. Sci.* **2020**, *504*, 144351. [DOI](#)
47. Di Bartolomeo, A. Graphene Schottky diodes: an experimental review of the rectifying graphene/semiconductor heterojunction. *Phys. Rep.* **2016**, *606*, 1-58. [DOI](#)
48. Kumari, P.; Bahadur, N.; Kong, L.; O'dell, L. A.; Merenda, A.; Dumée, L. F. Engineering Schottky-like and heterojunction materials for enhanced photocatalysis performance - a review. *Mater. Adv.* **2022**, *3*, 2309-23. [DOI](#)
49. Graimed, B. H.; Okab, A. A.; Jabbar, Z. H.; Issa, M. A.; Ammar, S. H. Highly stable β-Bi₂O₃/Ag decorated nanosilica as an efficient Schottky heterojunction for ciprofloxacin photodegradation in wastewater under LED illumination. *Mater. Sci. Semicond. Process.* **2022**, *156*, 107303. [DOI](#)
50. Manassero, A.; Satuf, M. L.; Alfano, O. M. Photocatalytic reactors with suspended and immobilized TiO₂: comparative efficiency

- evaluation. *Chem. Eng. J.* **2017**, *326*, 29-36. DOI
51. Joseph, A.; Vijayanandan, A. Review on support materials used for immobilization of nano-photocatalysts for water treatment applications. *Inorg. Chim. Acta.* **2023**, *545*, 121284. DOI
52. Goutham, R.; Badri Narayan, R.; Srikanth, B.; Gopinath, K. P. Supporting materials for immobilisation of nano-photocatalysts. In: Inamuddin, Sharma G, Kumar A, Lichtfouse E, Asiri AM, editors. Nanophotocatalysis and environmental applications. Cham: Springer International Publishing; 2019. pp. 49-82. DOI
53. Robert, D.; Keller, V.; Keller, N. Immobilization of a semiconductor photocatalyst on solid supports: methods, materials, and applications. In: Pichat P, editor. Photocatalysis and water purification. Wiley; 2013. pp. 145-78. DOI
54. Karavasili, M. V.; Tsakiroglou, C. D. Use of immobilized zinc oxide photocatalysts for wastewater treatment: application to methylene blue degradation. *Can. J. Chem. Eng.* **2022**, *100*, 893-910. DOI
55. Chairungsri, W.; Subkomkaew, A.; Kijjanapanich, P.; Chimupala, Y. Direct dye wastewater photocatalysis using immobilized titanium dioxide on fixed substrate. *Chemosphere* **2022**, *286*, 131762. DOI PubMed
56. Yusuf, A. O.; Mohamed, G. H.; Al-Sakkaf, R.; et al. Photocatalytic degradation of diclofenac amide in a fixed-bed reactor using TiO₂/β-Bi₂O₃: process optimization and stability analysis. *J. Photochem. Photobiol. A. Chem.* **2024**, *450*, 115470. DOI
57. Wetchakun, K.; Wetchakun, N.; Sakulsermsuk, S. An overview of solar/visible light-driven heterogeneous photocatalysis for water purification: TiO₂- and ZnO-based photocatalysts used in suspension photoreactors. *J. Ind. Eng. Chem.* **2019**, *71*, 19-49. DOI
58. Al-Tameemi, H. M.; Sukkar, K. A.; Abbar, A. H.; Kuraimid, Z. K. Optimization of photocatalytic process with SnO₂ catalyst for COD reduction from petroleum refinery wastewater using a slurry bubble photoreactor. *Case. Stud. Chem. Environ. Eng.* **2024**, *9*, 100687. DOI
59. Shokry, F.; El-Gedawy, M.; Nosier, S.; Abdel-Aziz, M. Optimizing photocatalytic degradation of methyl violet dye in a recirculating slurry-type reactor. *Results. Chem.* **2025**, *13*, 101980. DOI
60. Ng, K. H.; Chen, K.; Cheng, C. K.; Vo, D. N. Elimination of energy-consuming mechanical stirring: development of auto-suspending ZnO-based photocatalyst for organic wastewater treatment. *J. Hazard. Mater.* **2021**, *409*, 124532. DOI
61. Zheng, X.; Shen, Z.; Shi, L.; Cheng, R.; Yuan, D. Photocatalytic membrane reactors (PMRs) in water treatment: configurations and influencing factors. *Catalysts* **2017**, *7*, 224. DOI
62. Khader, E. H.; Mohammed, T. J.; Albayati, T. M.; et al. Current trends for wastewater treatment technologies with typical configurations of photocatalytic membrane reactor hybrid systems: a review. *Chem. Eng. Process.* **2023**, *192*, 109503. DOI
63. Samuel, O.; Othman, M. H. D.; Kamaludin, R.; et al. Treatment of oily wastewater using photocatalytic membrane reactors: a critical review. *J. Environ. Chem. Eng.* **2022**, *10*, 108539. DOI
64. Espíndola, J. C.; Cristóvão, R. O.; Mendes, A.; Boaventura, R. A.; Vilar, V. J. Photocatalytic membrane reactor performance towards oxytetracycline removal from synthetic and real matrices: suspended vs immobilized TiO₂-P25. *Chem. Eng. J.* **2019**, *378*, 122114. DOI
65. Nguyen, V.; Tran, Q. B.; Nguyen, X. C.; et al. Submerged photocatalytic membrane reactor with suspended and immobilized N-doped TiO₂ under visible irradiation for diclofenac removal from wastewater. *Process. Saf. Environ. Prot.* **2020**, *142*, 229-37. DOI
66. Janssens, R.; Hainaut, R.; Gillard, J.; Dailly, H.; Luis, P. Performance of a slurry photocatalytic membrane reactor for the treatment of real secondary wastewater effluent polluted by anticancer drugs. *Ind. Eng. Chem. Res.* **2021**, *60*, 2223-31. DOI
67. Amadelli, R.; Samiolo, L. Photoelectrocatalysis for water purification. In: Pichat P, editor. Photocatalysis and water purification. Wiley; 2013. pp. 241-70. DOI
68. Marinho, B. A.; Suhadolnik, L.; Likoza, B.; Huš, M.; Marinko, Ž.; Čeh, M. Photocatalytic, electrocatalytic and photoelectrocatalytic degradation of pharmaceuticals in aqueous media: analytical methods, mechanisms, simulations, catalysts and reactors. *J. Clean. Prod.* **2022**, *343*, 131061. DOI
69. Suhadolnik, L.; Pohar, A.; Novak, U.; Likoza, B.; Mihelič, A.; Čeh, M. Continuous photocatalytic, electrocatalytic and photoelectrocatalytic degradation of a reactive textile dye for wastewater-treatment processes: batch, microreactor and scaled-up operation. *J. Ind. Eng. Chem.* **2019**, *72*, 178-88. DOI
70. Meng, H.; Liu, Y.; Liu, P.; et al. Development of a three-dimensional photoelectrocatalytic reactor packed with granular sludge carbon photoelectrocatalyst for efficient wastewater treatment. *Sep. Purif. Technol.* **2021**, *277*, 119642. DOI
71. Boschetti, M.; Vincenzi, D.; Mangherini, G.; et al. Modular stand-alone photoelectrocatalytic reactor for emergent contaminant degradation via solar radiation. *Solar. Energy.* **2021**, *228*, 120-7. DOI
72. Sathya, K.; Nagarajan, K.; Carlin Geor Malar, G.; Rajalakshmi, S.; Raja Lakshmi, P. A comprehensive review on comparison among effluent treatment methods and modern methods of treatment of industrial wastewater effluent from different sources. *Appl. Water. Sci.* **2022**, *12*, 70. DOI PubMed PMC
73. Sacco, O.; Vaiano, V.; Sannino, D. Main parameters influencing the design of photocatalytic reactors for wastewater treatment: a mini review. *J. Chem. Technol. Biotechnol.* **2020**, *95*, 2608-18. DOI
74. Vaiano, V.; Sacco, O.; Pisano, D.; Sannino, D.; Ciambelli, P. From the design to the development of a continuous fixed bed photoreactor for photocatalytic degradation of organic pollutants in wastewater. *Chem. Eng. Sci.* **2015**, *137*, 152-60. DOI
75. Enesca, A. The influence of photocatalytic reactors design and operating parameters on the wastewater organic pollutants removal - a mini-review. *Catalysts* **2021**, *11*, 556. DOI
76. Shaghagh, M.; Sargazi, H.; Bazargan, A.; Bellardita, M. Photocatalytic reactor types and configurations. In: Bazargan A, editor. Photocatalytic water and wastewater treatment. IWA Publishing; 2022. pp. 73-110. DOI

77. Hakki, H. K.; Sillanpää, M. Comprehensive analysis of photocatalytic and photoreactor challenges in photocatalytic wastewater treatment: a case study with ZnO photocatalyst. *Mater. Sci. Semicond. Process.* **2024**, *181*, 108592. DOI
78. Asha, R. C.; Vishnuganth, M. A.; Remya, N.; Selvaraju, N.; Kumar, M. Livestock wastewater treatment in batch and continuous photocatalytic systems: performance and economic analyses. *Water. Air. Soil. Pollut.* **2015**, *226*, 2396. DOI
79. Wang, X.; Jia, J.; Wang, Y. Combination of photocatalysis with hydrodynamic cavitation for degradation of tetracycline. *Chem. Eng. J.* **2017**, *315*, 274-82. DOI
80. Alam, M. M.; Bin Mukhlis, M. Z.; Uddin, S.; et al. Photocatalytic degradation of reactive yellow in batch and continuous photoreactor using titanium dioxide. *J. Sci. Res.* **2012**, *4*, 665-74. DOI
81. Balarak, D.; Mostafapour, F. K. Photocatalytic degradation of amoxicillin using UV/synthesized NiO from pharmaceutical wastewater. *Indones. J. Chem.* **2019**, *19*, 211. DOI
82. Krishnan, T.; Wan, M. W. S. Photocatalytic degradation of dyes by TiO₂ process in batch photoreactor. *Lett. Appl. NanoBioSci.* **2020**, *9*, 1502-12. DOI
83. Colombo, E.; Ashokkumar, M. Comparison of the photocatalytic efficiencies of continuous stirred tank reactor (CSTR) and batch systems using a dispersed micron sized photocatalyst. *RSC. Adv.* **2017**, *7*, 48222-9. DOI
84. Yang, H.; Lee, Y. J.; Park, S. J.; Lee, C. G. Exploring the viability of a floating photocatalyst in a continuous stirred tank reactor system for continuous water treatment. *Environ. Sci. Pollut. Res. Int.* **2023**, *30*, 114582-90. DOI
85. Tang, C.; Chen, V. The photocatalytic degradation of reactive black 5 using TiO₂/UV in an annular photoreactor. *Water. Res.* **2004**, *38*, 2775-81. DOI
86. Ma, X.; Chen, X.; Yang, Y.; et al. Full-scale integrated skid-mounted plug flow photocatalytic reactor: treatment of hospital wastewater. *J. Environ. Chem. Eng.* **2024**, *12*, 111596. DOI
87. Adishkumar, S.; Kanmani, S.; Rajesh Banu, J.; Tae Yeom, I. Evaluation of bench-scale solar photocatalytic reactors for degradation of phenolic wastewaters. *Desalination. Water. Treat.* **2016**, *57*, 16862-70. DOI
88. Pedina, S.; Jena, H. M. Hydrodynamics of a three-phase annular fluidized bed photocatalytic reactor (TAFBPR) with TiO₂/CSGAC-experimental and statistical analysis. *Powder. Technol.* **2024**, *445*, 120124. DOI
89. Kumar Jaiswal, V.; Dutta Gupta, A.; Verma, V.; Sharan Singh, R. Degradation of p-cresol in the presence of UV light driven in an integrated system containing photocatalytic and packed bed biofilm reactor. *Bioresour. Technol.* **2023**, *387*, 129706. DOI
90. Wang, S.; Fu, X.; Wang, J.; Yan, M.; Xu, M.; Xu, C. Photocatalytic degradation of rhodamine B over Z-scheme photocatalyst BiFeO₃/3DOM-TiO_{2-x} in a fixed-bed reactor. *Mater. Sci. Semicond. Process.* **2024**, *173*, 108108. DOI
91. Alalm, M. G.; Djellabi, R.; Meroni, D.; Pirola, C.; Bianchi, C. L.; Boffito, D. C. Toward scaling-up photocatalytic process for multiphase environmental applications. *Catalysts* **2021**, *11*, 562. DOI
92. Kahveci, O.; Akkaya, A.; Sarıkaya, E. K.; et al. Construction of unary and ternary ZnO–CuO–CdO composite thin films and comprehensive analysis of their optical, electrical, and photocatalytic performance. *J. Alloys. Compd.* **2024**, *997*, 174827. DOI
93. Molinari, R.; Severino, A.; Lavorato, C.; Argurio, P. Which configuration of photocatalytic membrane reactors has a major potential to be used at an industrial level in tertiary sewage wastewater treatment? *Catalysts* **2023**, *13*, 1204. DOI
94. Janssens, R.; Mandal, M. K.; Dubey, K. K.; Luis, P. Slurry photocatalytic membrane reactor technology for removal of pharmaceutical compounds from wastewater: towards cytostatic drug elimination. *Sci. Total. Environ.* **2017**, *599-600*, 612-26. DOI PubMed
95. Rani, C. N.; Karthikeyan, S.; Prince Arockia Doss, S. Photocatalytic ultrafiltration membrane reactors in water and wastewater treatment - a review. *Chem. Eng. Process.* **2021**, *165*, 108445. DOI
96. Golshenas, A.; Sadeghian, Z.; Ashrafizadeh, S. N. Performance evaluation of a ceramic-based photocatalytic membrane reactor for treatment of oily wastewater. *J. Water. Process. Eng.* **2020**, *36*, 101186. DOI
97. Deeprecha, S.; Atfane, L.; Ayril, A.; Ogawa, M. Simple and efficient method for functionalizing photocatalytic ceramic membranes and assessment of its applicability for wastewater treatment in up-scalable membrane reactors. *Sep. Purif. Technol.* **2021**, *262*, 118307. DOI
98. Gomaa, H. G.; Zhou, W.; Zhu, J. Treatment of oily wastewater using submerged photocatalytic membrane reactor. *Particuology* **2024**, *94*, 252-60. DOI
99. Kubiak, A.; Ceglowski, M. Developing a novel continuous-flow cascade photocatalytic system for effective sulfamethoxazole elimination from hospital wastewater. *Chem. Eng. J.* **2024**, *495*, 153518. DOI
100. Zeghioud, H.; Kamagate, M.; Coulibaly, L. S.; Rtimi, S.; Assadi, A. A. Photocatalytic degradation of binary and ternary mixtures of antibiotics: reactive species investigation in pilot scale. *Chem. Eng. Res. Des.* **2019**, *144*, 300-9. DOI
101. Buehler, D.; Antenen, N.; Frei, M.; et al. Towards water and energy self-sufficiency: a closed-loop, solar-driven, low-tech laundry pilot facility (LaundReCycle) for the reuse of laundry wastewater. *Circ. Econ. Sust.* **2021**, *1*, 1037-51. DOI
102. Kayahan, E.; Jacobs, M.; Braeken, L.; et al. Dawn of a new era in industrial photochemistry: the scale-up of micro- and mesostructured photoreactors. *Beilstein. J. Org. Chem.* **2020**, *16*, 2484-504. DOI PubMed PMC
103. Hakke, V.; Sonawane, S.; Anandan, S.; Sonawane, S.; Ashokkumar, M. Process intensification approach using microreactors for synthesizing nanomaterials - a critical review. *Nanomaterials* **2021**, *11*, 98. DOI PubMed PMC
104. Abiev, R. S. Miniaturization as one of the paths to process intensification in chemical engineering. *Theor. Found. Chem. Eng.* **2020**, *54*, 1-2. DOI
105. Shukla, K.; Agarwalla, S.; Duraiswamy, S.; Gupta, R. K. Recent advances in heterogeneous micro-photoreactors for wastewater

- treatment application. *Chem. Eng. Sci.* **2021**, *235*, 116511. DOI
106. Peralta Muniz Moreira, R.; Li Puma, G. CFD modeling of pharmaceuticals and CECs removal by UV/H₂O₂ process in helical microcapillary photoreactors and evaluation of OH radical rate constants. *Chem. Eng. J.* **2021**, *415*, 128833. DOI
107. Kazemi Hakki, H.; Allahyari, S. Intensification of photocatalytic wastewater treatment using a novel continuous microcapillary photoreactor irradiated by visible LED lights. *Chem. Eng. Process.* **2022**, *175*, 108937. DOI
108. Russo, D.; Spasiano, D.; Vaccaro, M.; et al. Direct photolysis of benzoylcegonine under UV irradiation at 254 nm in a continuous flow microcapillary array photoreactor. *Chem. Eng. J.* **2016**, *283*, 243-50. DOI
109. Yusuf, A.; Oladipo, H.; Yildiz Ozer, L.; et al. Modelling of a recirculating photocatalytic microreactor implementing mesoporous N-TiO₂ modified with graphene. *Chem. Eng. J.* **2020**, *391*, 123574. DOI
110. Jia, L.; Jin, Y.; Li, J.; Wei, Z.; Chen, M.; Ma, J. Study on high-efficiency photocatalytic degradation of oxytetracycline based on a spiral microchannel reactor. *Ind. Eng. Chem. Res.* **2022**, *61*, 554-65. DOI
111. Zelić, I. E.; Tomašić, V.; Gomzi, Z. Development of a new rotating photocatalytic reactor for the degradation of hazardous pollutants. *Int. J. Chem. React. Eng.* **2023**, *21*, 823-33. DOI
112. Fallahizadeh, S.; Gholami, M.; Rahimi, M. R.; et al. The spinning disc reactor for photocatalytic degradation: a systematic review. *Heliyon* **2024**, *10*, e32440. DOI PubMed PMC
113. Fallahizadeh, S.; Rahimi, M. R.; Gholami, M.; Esrafil, A.; Farzadkia, M.; Kermani, M. Novel nanostructure approach for antibiotic decomposition in a spinning disc photocatalytic reactor. *Sci. Rep.* **2024**, *14*, 10566. DOI PubMed PMC
114. Ghasemi, A. H.; Zoqi, M. J.; Zanganeh Ranjbar, P. Enhanced photocatalytic degradation of methylene blue using a novel counter-rotating disc reactor. *Front. Chem.* **2024**, *12*, 1335180. DOI PubMed PMC
115. Yossry, A.; El-Ashtouky, E.; Abdel-Aziz, M.; Zatout, A.; Sedahmed, G. Intensification of the rate of diffusion-controlled reactions involved in wastewater treatment by using a rotating array of vertical cylinders reactor. *J. Environ. Chem. Eng.* **2022**, *10*, 107330. DOI
116. Borah, P.; Kumar, M.; Devi, P. Chapter 2 - Types of inorganic pollutants: metals/metalloids, acids, and organic forms. In: *Inorganic pollutants in water*. Elsevier; 2020. pp. 17-31. DOI
117. Zaynab, M.; Al-Yahyai, R.; Ameen, A.; et al. Health and environmental effects of heavy metals. *J. King. Saud. Univ. Sci.* **2022**, *34*, 101653. DOI
118. Tytla, M. Assessment of heavy metal pollution and potential ecological risk in sewage sludge from municipal wastewater treatment plant located in the most industrialized region in poland-case study. *Int. J. Environ. Res. Public. Health.* **2019**, *16*, 2430. DOI PubMed PMC
119. Sable, H.; Kumar, V.; Singh, V.; Rustagi, S.; Chahal, S.; Chaudhary, V. Strategically engineering advanced nanomaterials for heavy-metal remediation from wastewater. *Coord. Chem. Rev.* **2024**, *518*, 216079. DOI
120. Skliri, E.; Vamvasakis, I.; Papadas, I. T.; Choulis, S. A.; Armatas, G. S. Mesoporous composite networks of linked MnFe₂O₄ and ZnFe₂O₄ nanoparticles as efficient photocatalysts for the reduction of Cr(VI). *Catalysts* **2021**, *11*, 199. DOI
121. Li, Y.; Wang, S.; Guo, H.; et al. Synchronous removal of oxytetracycline and Cr(VI) in Fenton-like photocatalysis process driven by MnFe₂O₄/g-C₃N₄: performance and mechanisms. *Chemosphere* **2024**, *352*, 141371. DOI
122. Fatima, T.; Husain, S.; Khanuja, M. Superior photocatalytic and electrochemical activity of novel WS₂/PANI nanocomposite for the degradation and detection of pollutants: antibiotic, heavy metal ions, and dyes. *Chem. Eng. J. Adv.* **2022**, *12*, 100373. DOI
123. Qiu, F.; Pan, Y.; Tian, Y.; et al. The construction of large-aperture Schottky heterostructures and the study of the reduction properties of heavy metal ions under natural light. *Mater. Design.* **2025**, *250*, 113579. DOI
124. Mohamed, R. M.; Ismail, A. A. Photocatalytic reduction and removal of mercury ions over mesoporous CuO/ZnO S-scheme heterojunction photocatalyst. *Ceram. Int.* **2021**, *47*, 9659-67. DOI
125. Abbasi, H.; Salimi, F.; Golmohammadi, F. Removal of cadmium from aqueous solution by nano composites of bentonite/TiO₂ and bentonite/ZnO using photocatalysis adsorption process. *Silicon* **2020**, *12*, 2721-31. DOI
126. Sethy, N. K.; Arif, Z.; Mishra, P. K.; Kumar, P. Green synthesis of TiO₂ nanoparticles from Syzygium cumini extract for photocatalytic removal of lead (Pb) in explosive industrial wastewater. *Green. Process. Synth.* **2020**, *9*, 171-81. DOI
127. Liu, F.; Zhang, W.; Tao, L.; Hao, B.; Zhang, J. Simultaneous photocatalytic redox removal of chromium(VI) and arsenic(III) by hydrothermal carbon-sphere@nano-Fe₃O₄. *Environ. Sci. Nano.* **2019**, *6*, 937-47. DOI
128. Le, A. T.; Pung, S. Y.; Sreekantan, S.; Matsuda, A.; Huynh, D. P. Mechanisms of removal of heavy metal ions by ZnO particles. *Heliyon* **2019**, *5*, e01440. DOI PubMed PMC
129. Al-Sherbini, A. A.; Ghannam, H. E. A.; El-Ghanam, G. M. A.; El-Ella, A. A.; Youssef, A. M. Utilization of chitosan/Ag bionanocomposites as eco-friendly photocatalytic reactor for Bactericidal effect and heavy metals removal. *Heliyon* **2019**, *5*, e01980. DOI PubMed PMC
130. Zhang, P.; Li, H.; Wang, Y.; Song, J.; Huang, J.; Li, P. Highly efficient uranium (VI) remove from aqueous solution using nano-TiO₂-anchored polymerized dopamine-wrapped magnetic photocatalyst. *J. Clean. Prod.* **2023**, *425*, 138796. DOI
131. Dai, Z.; Zhen, Y.; Sun, Y.; Li, L.; Ding, D. ZnFe₂O₄/g-C₃N₄ S-scheme photocatalyst with enhanced adsorption and photocatalytic activity for uranium(VI) removal. *Chem. Eng. J.* **2021**, *415*, 129002. DOI
132. Liang, P.; Yuan, L.; Deng, H.; et al. Photocatalytic reduction of uranium(VI) by magnetic ZnFe₂O₄ under visible light. *Appl. Catal. B. Environ.* **2020**, *267*, 118688. DOI
133. Li, Z.; Zhang, Z.; Dong, Z.; et al. Synthesis of MoS₂/P-g-C₃N₄ nanocomposites with enhanced visible-light photocatalytic activity for

- the removal of uranium (VI). *J. Solid. State. Chem.* **2021**, *302*, 122305. DOI
134. Wang, J.; Wang, Y.; Wang, W.; et al. Tunable mesoporous g-C₃N₄ nanosheets as a metal-free catalyst for enhanced visible-light-driven photocatalytic reduction of U(VI). *Chem. Eng. J.* **2020**, *383*, 123193. DOI
135. Zhang, X.; Guo, R.; Wang, H.; Zhang, Z.; Chen, Y.; Zhang, Y. Enhanced synergistic removal of tetracycline and uranium in wastewater using Defective-Enriched S-scheme hollow dodecahedron K₃PW₁₂O₄₀@WS₂ heterojunction. *Chem. Eng. J.* **2024**, *495*, 153322. DOI
136. Xu, X.; Feng, L.; Cao, M.; et al. Z-Scheme heterojunction Cu₂(OH)₂F/Bi₂WO₆ with improved photocatalytic activity for uranium removal from wastewater under air atmosphere. *Sep. Purif. Technol.* **2024**, *350*, 128012. DOI
137. Ye, H.; Wen, R.; Wu, M.; et al. Tailor-Made Homo/Heterojunction engineering of CdS@Prussian blue via One-Pot kinetic regulation for photoreduction of uranium (VI) from radioactive wastewater. *Chem. Eng. J.* **2024**, *485*, 149731. DOI
138. Lu, S.; Yin, Y.; Bao, J.; et al. CdS@NiCr-LDH Z-scheme heterojunction with high adsorption-photocatalysis for uranium(VI) removal without any sacrificial agent. *J. Environ. Chem. Eng.* **2024**, *12*, 112989. DOI
139. Wu, P.; Yin, X.; Zhao, Y.; et al. Porphyrin-based hydrogen-bonded organic framework for visible light driven photocatalytic removal of U(VI) from real low-level radioactive wastewater. *J. Hazard. Mater.* **2023**, *459*, 132179. DOI
140. Chen, L.; Chen, B.; Kang, J.; et al. The synthesis of a novel conjugated microporous polymer and application on photocatalytic removal of uranium(VI) from wastewater under visible light. *Chem. Eng. J.* **2022**, *431*, 133222. DOI
141. Chakraborty, A. K.; Akter, S.; Ganguli, S.; Haque, M. A.; Nur, A. S.; Sabur, M. A. Design of FeWO₄@N-TiO₂ nanocomposite and its enhanced photocatalytic activity in decomposing methylene blue and phenol under visible light. *Environ. Technol. Innov.* **2024**, *33*, 103536. DOI
142. He, Q.; Si, S.; Song, L.; et al. Refractory petrochemical wastewater treatment by K₂S₂O₈ assisted photocatalysis. *Saudi. J. Biol. Sci.* **2019**, *26*, 849-53. DOI PubMed PMC
143. Alhajeri, N. S.; Tawfik, A.; Nasr, M.; Osman, A. I. Artificial intelligence-enabled optimization of Fe/Zn@biochar photocatalyst for 2,6-dichlorophenol removal from petrochemical wastewater: a techno-economic perspective. *Chemosphere* **2024**, *352*, 141476. DOI
144. Ramos-Huerta, L.; Aguilar-Martínez, O.; Piña-Pérez, Y.; et al. Effect of calcination temperature on CeO₂-based catalysts with enhanced photocatalytic degradation of phenol under UV light. *Mater. Sci. Semicond. Process.* **2025**, *187*, 109123. DOI
145. Alanazi, M. Q.; Virk, P.; Alterary, S. S.; et al. Effect of potential microplastics in sewage effluent on Nile Tilapia and photocatalytic remediation with zinc oxide nanoparticles. *Environ. Pollut.* **2023**, *332*, 121946. DOI
146. Martín-González, M.; Fernández-Rodríguez, C.; González-Díaz, O.; Susial, P.; Doña-Rodríguez, J. Open-cell ceramic foams covered with TiO₂ for the photocatalytic treatment of agro-industrial wastewaters containing imazalil at semi-pilot scale. *J. Taiwan. Inst. Chem. Eng.* **2023**, *147*, 104902. DOI
147. Khasawneh, O. F. S.; Palaniandy, P. Occurrence and removal of pharmaceuticals in wastewater treatment plants. *Process. Saf. Environ. Prot.* **2021**, *150*, 532-56. DOI
148. Cassini, A.; Högberg, L. D.; Plachouras, D.; et al; Burden of AMR Collaborative Group. Attributable deaths and disability-adjusted life-years caused by infections with antibiotic-resistant bacteria in the EU and the European Economic Area in 2015: a population-level modelling analysis. *Lancet. Infect. Dis.* **2019**, *19*, 56-66. DOI PubMed PMC
149. Konstas, P.; Kosma, C.; Konstantinou, I.; Albanis, T. Photocatalytic treatment of pharmaceuticals in real hospital wastewaters for effluent quality amelioration. *Water* **2019**, *11*, 2165. DOI
150. Ariza-Tarazona, M. C.; Villarreal-Chiu, J. F.; Barbieri, V.; Siligardi, C.; Cedillo-González, E. I. New strategy for microplastic degradation: green photocatalysis using a protein-based porous N-TiO₂ semiconductor. *Ceram. Int.* **2019**, *45*, 9618-24. DOI
151. Jeyavani, J.; Al-Ghanim, K. A.; Govindarajan, M.; Malafaia, G.; Vaseeharan, B. A convenient strategy for mitigating microplastics in wastewater treatment using natural light and ZnO nanoparticles as photocatalysts: a mechanistic study. *J. Contam. Hydrol.* **2024**, *267*, 104436. DOI PubMed
152. Sanchez, J. M.; Oliva, J.; Gomez-Solis, C.; et al. High removal of PS and PET microplastics from tap water by using Fe₂O₃ porous microparticles and photothermal irradiation with NIR light. *Chemosphere* **2024**, *367*, 143538. DOI
153. Chokejaroenrat, C.; Watcharatharapong, T.; T-Thienprasert, J.; et al. Decomposition of microplastics using copper oxide/bismuth vanadate-based photocatalysts: insight mechanisms and environmental impacts. *Mar. Pollut. Bull.* **2024**, *201*, 116205. DOI
154. Wu, F.; Yu, H.; Chang, F.; et al. Fabrication of a C₃N₄/Bi₁₂O₁₇Cl₂ heterojunction photocatalytic membrane applied for pharmaceutical and microplastic treatment. *Sep. Purif. Technol.* **2025**, *364*, 132394. DOI
155. Gu, M.; Duan, L.; Zhang, Z.; et al. Multi-charge bridge transfer guiding design of photocatalyst with oxygen defects for effective degradation of PFAS in fluoropolymer production wastewater. *Chem. Eng. J.* **2025**, *505*, 159124. DOI
156. Wen, Y.; Rentería-Gómez, Á.; Day, G. S.; et al. Integrated photocatalytic reduction and oxidation of perfluorooctanoic acid by metal-organic frameworks: key insights into the degradation mechanisms. *J. Am. Chem. Soc.* **2022**, *144*, 11840-50. DOI
157. Gates, K.; Rai, S.; Pramanik, A.; et al. Insight into the photocatalytic degradation mechanism for “Forever Chemicals” PFNA by reduced graphene oxide/WO₃ nanoflower heterostructures. *ACS. Omega.* **2025**, *10*, 10675-84. DOI PubMed PMC
158. Devi, A. P.; Padhi, D. K.; Madhual, A.; Mishra, P. M.; Behera, A. K. Plant biomass driven synthesis of gAu/RGO nanocomposite towards photocatalytic degradation of phenolic compounds in wastewater. *J. Environ. Chem. Eng.* **2023**, *11*, 110161. DOI
159. Abdelfattah, I.; Ismail, A. A. Reduction of COD concentration and complete removal of phenol in industrial wastewater utilizing mesoporous TiO₂ nanoparticles under UVA illumination. *Opt. Mater.* **2023**, *145*, 114410. DOI
160. Mahboob, I.; Shafiq, S.; Shafiq, I.; et al. Mesoporous LaVO₄/MCM-48 nanocomposite with visible-light-driven photocatalytic

- degradation of phenol in wastewater. *Environ. Res.* **2023**, *218*, 114983. DOI PubMed
161. Safaralizadeh, E.; Mahjoub, A.; Janitabardarzi, S. Visible light-induced degradation of phenolic contaminants utilizing nanoscale TiO₂ and ZnO impregnated with SR 7B (SR) dye as advanced photocatalytic systems. *Ceram. Int.* **2025**, *51*, 1958-69. DOI
 162. Rashtizadeh, A.; Delnavaz, M.; Samadi, A.; Heidarzadeh, N. Photodegradation of POPs-containing wastewater using sunlight driven Ce-doped-ZnO/g-C₃N₄ photocatalyst: optimization, and cost-efficiency analysis. *Chem. Phys. Lett.* **2023**, *811*, 140253. DOI
 163. Liang, Y.; Wang, B.; Li, S.; et al. Enhanced photocatalysis using metal-organic framework MIL-101(Fe) for crude oil degradation in oil-polluted water. *J. Fuel. Chem. Technol.* **2024**, *52*, 607-18. DOI
 164. Brindhadevi, K.; Kim, T. P.; Alharbi, S. A.; Ramesh, M. D.; Lee, J.; Bharathi, D. Enhanced photocatalytic degradation of polycyclic aromatic hydrocarbons (PAHs) using NiO nanoparticles. *Environ. Res.* **2024**, *252*, 118454. DOI PubMed
 165. Amakiri, K. T.; Angelis-Dimakis, A.; Chatzisyseon, E. Photocatalytic degradation of phenol and polycyclic aromatic hydrocarbons in water by novel acid soluble collagen-polyvinylpyrrolidone polymer embedded in nitrogen-TiO₂. *Chem. Phys.* **2025**, *589*, 112485. DOI
 166. Ghugal, S. G.; Vidyasagar, D.; Tadi, K. K.; et al. Optimized photocatalytic performance of ZnS-SnO₂ heterostructures for visible light driven mineralization of Acid violet 7 dye and inactivation of bacteria. *Mater. Sci. Semicond. Process.* **2023**, *165*, 107657. DOI
 167. Muñoz-Flores, P.; Poon, P. S.; Ania, C. O.; Matos, J. Performance of a C-containing Cu-based photocatalyst for the degradation of tartrazine: comparison of performance in a slurry and CPC photoreactor under artificial and natural solar light. *J. Colloid. Interface. Sci.* **2022**, *623*, 646-59. DOI
 168. Diego-Lopez, A.; Cabezuelo, O.; Vidal-Moya, A.; Marin, M. L.; Bosca, F. Synthesis and mechanistic insights of SiO₂@WO₃@Fe₃O₄ as a novel supported photocatalyst for wastewater remediation under visible light. *Appl. Mater. Today.* **2023**, *33*, 101879. DOI
 169. Alzahrani, F. M. A.; Anwar, M.; Farooq, A.; Alrowaili, Z.; Al-Buriah, M.; Warsi, M. F. A new BiOCl-ZnFe₂O₄/CNTs ternary composite for remarkable photocatalytic degradation studies of a herbicide and a diazo dye. *Opt. Mater.* **2024**, *148*, 114876. DOI
 170. Fiorenza, R.; Di Mauro, A.; Cantarella, M.; Privitera, V.; Impellizzeri, G. Selective photodegradation of 2,4-D pesticide from water by molecularly imprinted TiO₂. *J. Photochem. Photobiol. A. Chem.* **2019**, *380*, 111872. DOI
 171. Fenoll, J.; Garrido, I.; Flores, P.; et al. Implementation of a new modular facility to detoxify agro-wastewater polluted with neonicotinoid insecticides in farms by solar photocatalysis. *Energy* **2019**, *175*, 722-9. DOI
 172. Olatunde, O. C.; Onwudiwe, D. C. A comparative study of the effect of graphene oxide, graphitic carbon nitride, and their composite on the photocatalytic activity of Cu₃SnS₄. *Catalysts* **2022**, *12*, 14. DOI
 173. Vignati, D.; Lofrano, G.; Libralato, G.; et al. Photocatalytic ZnO-assisted degradation of spiramycin in urban wastewater: degradation kinetics and toxicity. *Water* **2021**, *13*, 1051. DOI
 174. Xu, Y.; Yang, X.; Liang, C.; Peng, L. Efficient adsorption and photocatalytic degradation of pharmaceutical compounds by Bi₂₄O₃₁Br₁₀: mechanism, toxicity assessment, and degradation pathways. *J. Water. Process. Eng.* **2025**, *71*, 107233. DOI
 175. Antonopoulou, M.; Papadaki, M.; Rapti, I.; Konstantinou, I. Photocatalytic degradation of pharmaceutical amisulpride using g-C₃N₄ catalyst and UV-A irradiation. *Catalysts* **2023**, *13*, 226. DOI
 176. Mohamed, Z. H.; Riyad, Y. M.; Hendawy, H. A.; Abdelbary, H. M. H. Enhanced photocatalytic degradation of the antidepressant sertraline in aqueous solutions by zinc oxide nanoparticles. *Water* **2023**, *15*, 2074. DOI
 177. Evgenidou, E.; Rapti, A.; Koronaiou, L.; Petromelidou, S.; Anagnostopoulou, K.; Lambropoulou, D. Photocatalytic degradation of the antidepressant drug bupropion. Performance, water matrix effect and identification of transformation products. *Sustain. Chem. Environ.* **2023**, *3*, 100028. DOI
 178. Chatzimpaloglou, A.; Christophoridis, C.; Nika, M. C.; et al. Degradation of antineoplastic drug etoposide in aqueous environment by photolysis and photocatalysis. Identification of photocatalytic transformation products and toxicity assessment. *Chem. Eng. J.* **2022**, *431*, 133969. DOI
 179. Berbentea, A.; Ciopec, M.; Duteanu, N.; et al. Advanced photocatalytic degradation of cytarabine from pharmaceutical wastewaters. *Toxics* **2024**, *12*, 405. DOI PubMed PMC
 180. Swedha, M.; Alatar, A. A.; Okla, M. K.; et al. Graphitic carbon nitride embedded Ni₃(VO₄)₂/ZnCr₂O₄ Z-scheme photocatalyst for efficient degradation of p-chlorophenol and 5-fluorouracil, and genotoxic evaluation in Allium cepa. *J. Ind. Eng. Chem.* **2022**, *112*, 244-57. DOI
 181. Yasir, M.; Ali, H.; Masar, M.; et al. Design and fabrication of TiO₂/Nd polyurethane nanofibers based photoreactor: a continuous flow kinetics study for Estril degradation and mechanism. *J. Water. Process. Eng.* **2023**, *56*, 104271. DOI
 182. Ali, H.; Yasir, M.; Ngwabebhoh, F. A.; et al. Boosting photocatalytic degradation of estrone hormone by silica-supported g-C₃N₄/WO₃ using response surface methodology coupled with Box-Behnken design. *J. Photochem. Photobiol. A. Chem.* **2023**, *441*, 114733. DOI
 183. Ruta, V.; Sivo, A.; Bonetti, L.; Bajada, M. A.; Vilé, G. Structural effects of metal single-atom catalysts for enhanced photocatalytic degradation of gemfibrozil. *ACS. Appl. Nano. Mater.* **2022**, *5*, 14520-8. DOI PubMed PMC
 184. Mar-Ortiz, A. F.; Salazar-Rábago, J. J.; Sánchez-Polo, M.; Rozalen, M.; Cerino-Córdova, F. J.; Loredó-Cancino, M. Photodegradation of antihistamine chlorpheniramine using a novel iron-incorporated carbon material and solar radiation. *Environ. Sci. Water. Res. Technol.* **2020**, *6*, 2607-18. DOI
 185. Sehrawat, P.; Raj, A.; Singh, S.; Mehta, S. K.; Bhinder, S. S.; Kansal, S. K. Solar-driven S-scheme Zn_{0.5}Cd_{0.5}S/MoS₂ composite for photocatalytic ketorolac tromethamine degradation and hydrogen generation coupled with benzyl alcohol oxidation. *Int. J. Hydrogen. Energy.* **2024**, *62*, 17-30. DOI

186. Alomar, M. S.; Bakather, O. Y.; Zouli, N.; et al. Solar-driven purification: removing pharmaceutical contaminants from water using carbon-doped NASICON photocatalyst. *Mater. Sci. Semicond. Process.* **2025**, *185*, 108901. DOI
187. Galaburda, M.; Nazarkovsky, M.; Osipiuk, K.; et al. Enhanced photocatalytic degradation of antiviral drugs lopinavir and ritonavir by Ni doped ZnO/SiO₂ nanocomposites. *J. Environ. Chem. Eng.* **2024**, *12*, 114525. DOI
188. Hojamberdiev, M.; Czech, B.; Wasilewska, A.; et al. Detoxifying SARS-CoV-2 antiviral drugs from model and real wastewaters by industrial waste-derived multiphase photocatalysts. *J. Hazard. Mater.* **2022**, *429*, 128300. DOI PubMed PMC
189. Kowalczyk, A.; Zgardzińska, B.; Osipiuk, K.; et al. The visible-light-driven activity of biochar-doped TiO₂ photocatalysts in β -blockers removal from water. *Materials* **2023**, *16*, 1094. DOI PubMed PMC
190. Sarabyar, S.; Farahbakhsh, A.; Tahmasebi, H. A.; Mahmoodzadeh, V. B.; Khosroyar, S. Enhancing photocatalytic degradation of beta-blocker drugs using TiO₂ NPs/zeolite and ZnO NPs/zeolite as photocatalysts: optimization and kinetic investigations. *Sci. Rep.* **2024**, *14*, 27390. DOI PubMed PMC
191. Luo, Y.; Feng, L.; Liu, Y.; Zhang, L. Disinfection by-products formation and acute toxicity variation of hospital wastewater under different disinfection processes. *Sep. Purif. Technol.* **2020**, *238*, 116405. DOI
192. Majumder, A.; Gupta, A. K.; Ghosal, P. S.; Varma, M. A review on hospital wastewater treatment: a special emphasis on occurrence and removal of pharmaceutically active compounds, resistant microorganisms, and SARS-CoV-2. *J. Environ. Chem. Eng.* **2021**, *9*, 104812. DOI PubMed PMC
193. Zhang, G.; Li, W.; Chen, S.; Zhou, W.; Chen, J. Problems of conventional disinfection and new sterilization methods for antibiotic resistance control. *Chemosphere* **2020**, *254*, 126831. DOI
194. Zhan, J.; Xu, S.; Zhu, Y.; et al. Potential pathogenic microorganisms in rural wastewater treatment process: succession characteristics, concentration variation, source exploration, and risk assessment. *Water. Res.* **2024**, *254*, 121359. DOI
195. Chen, P.; Yu, X.; Zhang, J. Photocatalysis enhanced constructed wetlands effectively remove antibiotic resistance genes from domestic wastewater. *Chemosphere* **2023**, *325*, 138330. DOI
196. Saravanan, A.; Kumar, P. S.; Jeevanantham, S.; Karishma, S.; Kiruthika, A. Photocatalytic disinfection of micro-organisms: mechanisms and applications. *Environ. Technol. Innov.* **2021**, *24*, 101909. DOI
197. Baaloudj, O.; Assadi, I.; Nasrallah, N.; El Jery, A.; Khezami, L.; Assadi, A. A. Simultaneous removal of antibiotics and inactivation of antibiotic-resistant bacteria by photocatalysis: a review. *J. Water. Process. Eng.* **2021**, *42*, 102089. DOI
198. Channa, N.; Gadhi, T. A.; Mahar, R. B.; Chiadò, A.; Bonelli, B.; Tagliaferro, A. Combined photocatalytic degradation of pollutants and inactivation of waterborne pathogens using solar light active α/β -Bi₂O₃. *Colloids. Surf. A.* **2021**, *615*, 126214. DOI
199. Jaffari, Z. H.; Lam, S.; Sin, J.; Zeng, H.; Mohamed, A. R. Magnetically recoverable Pd-loaded BiFeO₃ microcomposite with enhanced visible light photocatalytic performance for pollutant, bacterial and fungal elimination. *Sep. Purif. Technol.* **2020**, *236*, 116195. DOI
200. Achouri, F.; Said, M. B.; Wahab, M. A.; et al. Effect of photocatalysis (TiO₂/UV_A) on the inactivation and inhibition of *Pseudomonas aeruginosa* virulence factors expression. *Environ. Technol.* **2021**, *42*, 4237-46. DOI PubMed
201. Krishnan, S.; Zulkapli, N. S.; Din, M. F. B. M.; Majid, Z. A.; Nasrullah, M.; Sairan, F. M. Photocatalytic degradation of methylene blue dye and fungi *Fusarium equiseti* using titanium dioxide recovered from drinking water treatment sludge. *Biomass. Conv. Bioref.* **2023**, *13*, 10853-63. DOI
202. Abeledo-Lameiro, M. J.; Polo-López, M. I.; Ares-Mazás, E.; Gómez-Couso, H. Inactivation of the waterborne pathogen *Cryptosporidium parvum* by photo-Fenton process under natural solar conditions. *Appl. Catal. B. Environ.* **2019**, *253*, 341-7. DOI
203. Leonel, L. P.; Tonetti, A. L. Action of chlorine, peracetic acid, UV-LED radiation, and advanced oxidation process on *Giardia lamblia* cysts for reclaimed water production. *Int. J. Environ. Sci. Technol.* **2025**, *22*, 7783-96. DOI
204. Baudys, M.; Sopha, H.; Hodek, J.; et al. Inactivation of influenza virus as representative of enveloped RNA viruses on photocatalytically active nanoparticle and nanotubular TiO₂ surfaces. *Catal. Today.* **2024**, *430*, 114511. DOI
205. Zhang, C.; Xiong, W.; Li, Y.; Lin, L.; Zhou, X.; Xiong, X. Continuous inactivation of human adenoviruses in water by a novel g-C₃N₄/WO₃/biochar memory photocatalyst under light-dark cycles. *J. Hazard. Mater.* **2023**, *442*, 130013. DOI PubMed
206. Zhang, L.; Xi, T.; Zhu, D.; et al. Adsorption-enhanced photocatalytic waterborne virus inactivation by graphite carbon nitride conjugated with covalent organic frameworks. *Chem. Eng. J.* **2023**, *472*, 144893. DOI
207. Xie, Y.; Zhang, Z.; Zhao, Y.; Han, Y.; Liu, C.; Sun, Y. Effect of dissolved organic matter on the inactivation of bacteriophage MS₂ by graphitic carbon nitride - based photocatalysis. *J. Environ. Chem. Eng.* **2024**, *12*, 112025. DOI
208. Lee, J.; Kim, J.; Kim, S.; et al. Enhanced virucidal activity of facet-engineered Cu-doped TiO₂ nanorods under visible light illumination. *Water. Res.* **2025**, *268*, 122579. DOI
209. Cheng, R.; Kang, M.; Shen, Z. P.; Shi, L.; Zheng, X. Visible-light-driven photocatalytic inactivation of bacteriophage f2 by Cu-TiO₂ nanofibers in the presence of humic acid. *J. Environ. Sci.* **2019**, *77*, 383-91. DOI
210. Jacob, M. F.; Quiberoni, A. D. L.; Alfano, O. M.; Ballari, M. D. L. M.; Briggiler Marcó, M. Photocatalytic paint for phage inactivation in dairy industry: inactivation constants and efficiencies. *J. Environ. Chem. Eng.* **2023**, *11*, 110617. DOI
211. Lin, Z.; Ye, S.; Xu, Y.; et al. Construction of a novel efficient Z-scheme BiVO₄/EAQ heterojunction for the photocatalytic inactivation of antibiotic-resistant pathogens: performance and mechanism. *Chem. Eng. J.* **2023**, *453*, 139747. DOI
212. Yang, J.; Luo, H.; Zhu, X.; et al. Copper-doped bismuth oxychloride nanosheets assembled into sphere-like morphology for improved photocatalytic inactivation of drug-resistant bacteria. *Sci. Total. Environ.* **2024**, *912*, 168916. DOI
213. Zhong, J.; Ahmed, Y.; Carvalho, G.; et al. Simultaneous removal of micropollutants, antibiotic resistant bacteria, and antibiotic

- resistance genes using graphitic carbon nitride under simulated solar irradiation. *Chem. Eng. J.* **2022**, *433*, 133839. DOI
214. Zhou, Z.; Shen, Z.; Cheng, Z.; et al. Mechanistic insights for efficient inactivation of antibiotic resistance genes: a synergistic interfacial adsorption and photocatalytic-oxidation process. *Sci. Bull.* **2020**, *65*, 2107-19. DOI
215. Ye, S.; Xu, Y.; Huang, L.; et al. MWCNT/BiVO₄ photocatalyst for inactivation performance and mechanism of *Shigella flexneri* HL, antibiotic-resistant pathogen. *Chem. Eng. J.* **2021**, *424*, 130415. DOI
216. Osman, A. I.; Elgarahy, A. M.; Eltaweil, A. S.; et al. Biofuel production, hydrogen production and water remediation by photocatalysis, biocatalysis and electrocatalysis. *Environ. Chem. Lett.* **2023**, *21*, 1315-79. DOI
217. Zeng, Q.; An, W.; Peng, D.; et al. Research progress in photocatalytic-coupled microbial electrochemical technology in wastewater treatment. *Catalysts* **2025**, *15*, 81. DOI
218. Xiao, J.; Xie, Y.; Rabeah, J.; Brückner, A.; Cao, H. Visible-light photocatalytic ozonation using graphitic C₃N₄ catalysts: a hydroxyl radical manufacturer for wastewater treatment. *Acc. Chem. Res.* **2020**, *53*, 1024-33. DOI
219. Rodríguez, E. M.; Rey, A.; Mena, E.; Beltrán, F. J. Application of solar photocatalytic ozonation in water treatment using supported TiO₂. *Appl. Catal. B. Environ.* **2019**, *254*, 237-45. DOI
220. Jiad, M. M.; Abbar, A. H. Petroleum refinery wastewater treatment using a novel combined electro-Fenton and photocatalytic process. *J. Ind. Eng. Chem.* **2024**, *129*, 634-55. DOI
221. Xu, P.; Xu, H.; Zheng, D. Simultaneous electricity generation and wastewater treatment in a photocatalytic fuel cell integrating electro-Fenton process. *J. Power. Sources.* **2019**, *421*, 156-61. DOI
222. Serrà, A.; Gómez, E.; Michler, J.; Philippe, L. Facile cost-effective fabrication of Cu@Cu₂O@CuO-microalgae photocatalyst with enhanced visible light degradation of tetracycline. *Chem. Eng. J.* **2021**, *413*, 127477. DOI
223. Li, C.; Tian, Q.; Zhang, Y.; et al. Sequential combination of photocatalysis and microalgae technology for promoting the degradation and detoxification of typical antibiotics. *Water. Res.* **2022**, *210*, 117985. DOI
224. Lu, Z.; Xu, Y.; Peng, L.; Liang, C.; Liu, Y.; Ni, B. J. A two-stage degradation coupling photocatalysis to microalgae enhances the mineralization of enrofloxacin. *Chemosphere* **2022**, *293*, 133523. DOI
225. de Sousa, C. M.; Cardoso, V. L.; Batista, F. R. X. A coupled photocatalytic system using niobium oxide and microalgae: Cr (VI)-contaminated wastewater treatment. *J. Photochem. Photobiol. A. Chem.* **2023**, *439*, 114602. DOI
226. Wang, G.; Cheng, H. Application of photocatalysis and sonocatalysis for treatment of organic dye wastewater and the synergistic effect of ultrasound and light. *Molecules* **2023**, *28*, 3706. DOI PubMed PMC
227. Schieppati, D.; Galli, F.; Peyot, M. L.; Yargeau, V.; Bianchi, C. L.; Boffito, D. C. An ultrasound-assisted photocatalytic treatment to remove an herbicidal pollutant from wastewaters. *Ultrason. Sonochem.* **2019**, *54*, 302-10. DOI PubMed
228. Karim, A. V.; Shriwastav, A. Degradation of ciprofloxacin using photo, sono, and sonophotocatalytic oxidation with visible light and low-frequency ultrasound: degradation kinetics and pathways. *Chem. Eng. J.* **2020**, *392*, 124853. DOI
229. Khalegh, R.; Qaderi, F. Optimization of the effect of nanoparticle morphologies on the cost of dye wastewater treatment via ultrasonic/photocatalytic hybrid process. *Appl. Nanosci.* **2019**, *9*, 1869-89. DOI
230. Chen, P.; Yu, X.; Zhang, J.; Wang, Y. New and traditional methods for antibiotic resistance genes removal: constructed wetland technology and photocatalysis technology. *Front. Microbiol.* **2022**, *13*, 1110793. DOI PubMed PMC
231. Nguyen, H. T. T.; Chao, H.; Chen, K. Treatment of organic matter and tetracycline in water by using constructed wetlands and photocatalysis. *Appl. Sci.* **2019**, *9*, 2680. DOI
232. Başaran Dindaş, G.; Çalışkan, Y.; Çelebi, E. E.; Tekbaş, M.; Bektaş, N.; Yatmaz, H. C. Treatment of pharmaceutical wastewater by combination of electrocoagulation, electro-fenton and photocatalytic oxidation processes. *J. Environ. Chem. Eng.* **2020**, *8*, 103777. DOI
233. Aldana, J. C.; Acero, J. L.; Álvarez, P. M. Membrane filtration, activated sludge and solar photocatalytic technologies for the effective treatment of table olive processing wastewater. *J. Environ. Chem. Eng.* **2021**, *9*, 105743. DOI
234. Kusworo, T. D.; Purwanto, P.; Jos, B.; et al. Photocatalytic nanohybrid UV-light-driven PVDF/GO-NiFe@SiO₂ membrane coupled with bentonite adsorption and ozonation process for a sustainable textile wastewater treatment. *Process. Saf. Environ. Prot.* **2024**, *190*, 438-57. DOI
235. Majumder, A.; Otter, P.; Röher, D.; et al. Combination of advanced biological systems and photocatalysis for the treatment of real hospital wastewater spiked with carbamazepine: a pilot-scale study. *J. Environ. Manage.* **2024**, *351*, 119672. DOI